NBSIR 74-605

Crush Characteristics of Automobile Structural Components

Donald C. Robinson

Engineering Mechanics Section
Mechanics Division
Institute for Basic Standards
National Bureau of Standards
Washington, D. C. 20234

January 1975

Final Report

Prepared for
National Highway Traffic Safety Administration
Department of Transportation
400 7th Street, S.W.
Washington, D. C. 20590

NBSIR 74–605

CRUSH CHARACTERISTICS OF AUTOMOBILE STRUCTURAL COMPONENTS

Donald C. Robinson

Engineering Mechanics Section
Mechanics Division
Institute for Basic Standards
National Bureau of Standards
Washington, D. C. 20234

January 1975

Final Report

Prepared for
National Highway Traffic Safety Administration
Department of Transportation
400 7th Street, S.W.
Washington, D.C. 20590

U. S. DEPARTMENT OF COMMERCE, Frederick B. Dent, Secretary

NATIONAL BUREAU OF STANDARDS, Richard W. Roberts, Director

CONTENTS

Crush Characteristics of Automobile Structural Components

Donald C. Robinson

ABSTRACT

Static and dynamic test procedures were developed for evaluating the crush characteristics of automotive structural components which perform a major structural function in side impacts. Laboratory tests were conducted on several 1969 to 1971 4-door intermediate size automobiles to evaluate the crush characteristics of some of their structural components. Static crush tests were conducted in the 12-million-lbf capacity universal testing machine at the National Bureau of Standards, employing its large working space. The dynamic tests were conducted using the monorails attached to the sensitive crosshead and the tie-down floor system which is incorporated in the foundation of this machine. The crush loads were applied perpendicular to the vehicle side for each of the tests. The response of the structural components was established based on the evaluation of displacement and/or strain measurements and detailed examination of the permanently deformed components following each test. Empirical factors were obtained which are useful for comparison of static and dynamic crush characteristics of a vehicle side door structure over a limited loading range. Further development of the test procedures is required in order to extend the range over which such results would be meaningful.

Key Words: Automobile side impact, crush characteristics, displacement measurements, door structure, drop tests, dynamic crush tests, impact collisions, plastic deformation, static crush tests, strain measurements, structural components, test procedures.

1. INTRODUCTION

Automobile collisions in which loads are developed that result in permanent deformation of a vehicle side structure account for a

significant number of injury producing accidents each year [1, 2]. Accident data reveal that side impacts are more severe in causing dangerous or fatal injuries than other accident types. The objective of the research described in this report was to develop methods for evaluating the crush characteristics of the principal components which perform a major structural function in a vehicle whose side is struck by another vehicle.

While emphasis was placed on developing laboratory procedures for characterizing the static and dynamic crushing of various structural components, the data obtained from a limited number of tests provide additional general information which may be useful in the development of computer simulation programs for vehicle side impacts. The component crush characteristics are given in terms of load-deformation relationships and, for several cases, in terms of the relative deformation between members. Analyses of the static test data indicate significant structural degrees of freedom for various components. The regions of localized plastic deformation for the components are identified and some insight is provided into the sequence in which forces are developed in various members during application of the crush loads.

The static and dynamic loads applied to two vehicles, which were identical in design and similar in condition, were correlated at selected values of their side door deformation. Empirical factors which were obtained are useful for comparison of the static and dynamic crush characteristics of a vehicle side door structure over a limited loading range. Further development of the test procedures required to extend the range of these factors is discussed, and recommendations for obtaining similar results for additional components are made.

In accordance with NBS policy, the brand names of commercial products tested are not given in this report. Consequently the three vehicles tested are identified by the letters A, B and C.

2. DESIGN OF SIMULATED BUMPER

In order to evaluate the crush characteristics of the automotive structural members which perform a major function during side impact collisions, a contoured bumper was fabricated to simulate the front of an impacting vehicle. A review of the crashworthiness research literature indicated that the basis existed for the design of a realistic bumper which could provide a repeatable test technique [1, 2]. The configuration chosen was designed so that no permanent deformation would occur in its members during static or dynamic crush tests.

---

[1] Numerals in brackets refer to references found at the end of this report.

The simulated bumper used for the static crush tests is shown in Figure 1. This design is essentially identical to that specified in the Society of Automotive Engineers (SAE) recommended practice for moving barrier collision tests, insofar as the contoured face is designated [3]. The SAE design was based on deformation considerations and observations of a wide range of side impacts from a wide range of vehicles. The support structure was designed so that all parts of the loading system would be rigid with respect to the structure to be crushed so that no yielding would occur in its components. The weight of the bumper in this configuration was about 800 lb (363 kg).

3. UNIVERSAL TESTING MACHINE

In order to apply the static crush loads to the vehicle side structures, it was decided to employ the 12-million-lbf capacity universal testing machine at the National Bureau of Standards because of its large working space [4]. A photograph of this machine is shown in Figure 2. The simulated bumper described in the previous section was attached to the sensitive crosshead of this machine for the static tests, during which the vehicle support frame was attached to the machine platen. For the dynamic tests, it was found convenient to use the monorails attached to the machine sensitive crosshead from which to drop the bumper onto the vehicle side. The vehicle support frame was attached to the tie-down floor system which is incorporated in the foundation of this machine during the drop tests.

4. VEHICLE SUPPORT FRAME

In order to support the vehicles in the testing machine during static tests and on the machine tie-down floor for the drop tests, it was necessary to construct a frame structure for a vehicle so it could be oriented perpendicular to its usual position. The test frame was constructed using 12 inch steel I-beams which were reinforced by welding steel plates where the beams joined. Subsequent to the first several tests, the stiffness of several members was increased by welding additional plates to their flanges and improving the connections in order to support larger test loads.

The principal considerations for connecting the support frame to the vehicle were that it be rigid and not alter the characteristics of the side structural members being tested [5]. Consequently, the frame was attached to the vehicle underbody near the engine mounts and near the trunk. Because of the relatively stronger underbody construction for the "B" vehicles, it was possible to attach the frame relatively closer to the underbody than for Vehicle "A". Once the frame was installed in the test machine, the ends of the I-beam frame members in contact with the machine platen or the tie-down floor system were secured by clamping them to tie down points.

In addition, hydraulic jacks were placed under the axle hubs of the vehicle to prevent excessive canting of the vehicle as the side load was applied. Cables were used to restrain the vertical members of the support frame from excessive deflection during the test. A photograph showing Vehicle "A" mounted in the test frame and positioned in the testing machine for a static test is given in Figure 3.

5. TEST VEHICLE PREPARATION

General characteristics of the vehicles in the test program are listed in Table 1. In preparation for the static and dynamic tests, a number of non-load bearing parts of the vehicles were removed to reduce the handling weight, for safety, and for convenience in instrumenting the vehicle. The vehicles were first weighed on a precision mechanical scale. After weighing, the engine, transmission, fuel tank, side window glass and sealed beam lights were removed.

Interior trim items removed included the handles, the trim panels and window mechanisms for the front and rear doors, and the head rests and safety belt hardware attached to the floor. Components removed from the roof were the sun visors, shoulder harness assemblies, the headlining and headlining support rods. Although the rear window was removed from Vehicle "A", which was tested initially, the window was left in Vehicle "B-1" since the rear window frame carried some shearing loads during the first tests.

Strain gage locations were selected on the pillars, roof and sill, and door side guard beams. At these locations, the existing paint was removed in order to attach the gages to the parent metal surface. These locations were masked and the surrounding metal and the doors were painted with several shades of flat grey paint to improve the contrast and to reduce glare from lights when photographing the various components.

6. STATIC TEST PROCEDURES

6.1 Alignment of Simulated Bumper

The surface area over which crush loads were applied to a vehicle side with the simulated bumper was established from the following considerations: a) the determination of a reference point on the side structure and b) alignment of the bumper with respect to that reference. The position used for the reference was the Seating Reference Point, referred to hereafter as SRP, which corresponds to the driver's hip pivot point. This location, given with respect to the front seat belt anchorage locations, was obtained for each vehicle through the assistance of the Automotive Manufacturer's Association. After locating the SRP, it was marked by use of a circular target glued to the exterior surface of the front door.

Alignment of the bumper relative to the SRP was chosen to achieve a deformed side structure profile which would be representative of the profiles generated in perpendicular side impact collisions [2]. In selecting the bumper alignment, it is useful to measure the relative position of the front and side structure of two vehicles having the same design and weight, such as shown in Figure 4. After considering these factors, it was decided to align the axis through the center of the top edge of the steel band incorporated on the bumper face with the horizontal axis through the SRP, and aligning the center of the bumper with the vertical axis through the SRP location. This alignment was checked by use of plumb bobs which were suspended from the bumper after it was connected to the sensitive crosshead of the testing machine and the vehicle and test frame were moved onto the machine platen. After alignment of the vehicle relative to the bumper was completed, the test frame was rigidly connected to the tie down points available in the platen.

6.2 Static Test Instrumentation

The responses of the test vehicles to the static crush loads were determined by measurement of deformation and strain at selected locations on the structural components. Two types of transducers were used to measure deformation during the static tests: linear variable differential transformers (LVDT's) and potentiometer transducers consisting of a flexible steel cable wound on a precision reel coupled to a potentiometer having a nonlinearity of less than one percent. A photograph showing an LVDT and three cable transducers is shown in Figure 5.

The direct current LVDT sensors were calibrated using a calibrating stand with a micrometer. The maximum nonlinearity of these devices was 0.5 percent of full scale. Their resolution is limited only by the read-out equipment which is employed. The displacement range for these transducers was 1 to 2 inches (2.54 to 5.08 cm). For the larger range potentiometer transducers, a different calibration procedure was required. It was noted that several of the hydraulic testing machines in the laboratory had pacing dials which can be used for conducting mechanical tests at constant crosshead speeds. These dials were graduated and had a range of approximately 10 inches (25.4 cm). To calibrate a potentiometer transducer, the transducer was connected between the fixed and moving crossheads of a testing machine and the cable motion was controlled by operating the machine using the pacing dial for a displacement reference. The pacing dial readings were checked with a dial gage and were repeatable within .006 in (.15 mm) over the range checked. Since the potentiometer transducers had a range of up to 2 feet (0.61 m), it was required that their calibration be performed over several shorter ranges. The resolution of these transducers

was less than 0.5 percent of full scale. The errors of the displacement transducers were well within the SAE recommended practice guidelines.*

The strain gages employed were 120 ohm foil gages with encapsulated grids having a length of 0.25 inch (0.63 cm). They were attached in a single arm configuration at various positions and directions on the vehicle door structure back-up members, such as the pillars, sill and roof, and on the door side guard beams, dash and front glass.

6.3 Measurement Procedure

The displacement transducers were connected to the structural members by several different methods. Whenever possible, a small hole was drilled into the sheet metal and a self-locking screw was used to attach a fixture for supporting the end of the transducer cable. Where this procedure could weaken a member or otherwise interfere with the measurement, an adhesive was used to attach the fixtures. The displacement transducers were connected to signal conditioning and their output was digitized and recorded on a multichannel data acquisition system. The strain gages were connected to form a bridge circuit using signal conditioning within the data acquisition system and their output was similarly recorded. Other quantities recorded were a signal from a potentiometer in the testing machine console, whose output was directly proportional to the load indicator dial, and the power supply voltage for the transducer signal conditioning.

The static crush tests were conducted using the testing machine hydraulic controls to load the vehicle side with the simulated bumper which was attached to the machine sensitive crosshead. Load, displacement and strain data were recorded during the test on both paper and magnetic tape at load increments of several thousand pounds. The short range displacement transducers were reset whenever necessary, while the load was held constant, to ensure that their range was not exceeded. The data printed out on paper tape were spot checked during the test and visual observations were also recorded on this tape. The magnetic tape was processed after the test by a high speed digital computer in order to list the data in tabular form for convenience when performing a more thorough data reduction.

7. DYNAMIC TEST PROCEDURES

7.1 Modification of Bumper

In order to simulate the loading of an intermediate size 4 door sedan for the drop tests, the weight of the simulated bumper was increased

---

*e.g., Society of Automotive Engineers Recommended Practices SAE J211a and SAE J367.

to about 4100 lb (1860 kg) by the addition of lead. A steel block was first welded to the rear surface of the bumper face plate to provide for the mounting of several accelerometers. In order to keep this surface intact as molten lead was added, a tubular member surrounding the accelerometer mounting block was welded in place. Sheet metal containers were fabricated and attached to the bumper by brackets welded to the tubular members of the bumper, and molten lead was then poured into the containers. A photograph of the modified bumper after solidification of the lead is shown in Figure 6.

7.2 Instrumentation for Dynamic Tests

For computing the load applied by the simulated bumper for the drop tests, two types of accelerometers were attached to the steel block welded behind the face plate of the bumper. The primary transducer was a linear piezoresistive accelerometer designed specifically for automotive crash test applications and having a sensitivity of about 20 millivolts/g. Its full bridge design featured semiconductor elements connected in one side of a bridge and fixed precision resistors for internal bridge completion and shunt calibration. The low resistance of the piezoresistive transducers minimize electrostatic problems due to cable motion which have been encountered with higher resistance accelerometers whenever long cable lengths are required. The cable-accelerometer interface used recessed solder terminals. In order to further minimize any effects of cable motion, the terminal recess was filled with a silicone-rubber compound and the transducer cable was taped to the bumper at several locations near the transducer.

The secondary transducer was a piezoelectric transducer, having built-in signal conditioning, with a sensitivity of about 19 millivolts/g. This transducer was rugged but did not respond as well as the piezoresistive accelerometer at low frequencies. The battery supply required for this device was rigidly connected to the simulated bumper.

Prior to instrumenting the test vehicles, several experiments were conducted to determine the capability of the potentiometer transducers to survive and respond rapidly when subjected to the high speed displacements generated during the impact test. It was determined that neither the commercial nor the NBS developed transducers could respond fast enough unless the cables were extended, rather than being retracted as during the static tests. Since the NBS developed transducers of the type shown in Figure 5 were more rugged than the commercial devices, they were chosen for this purpose. It was necessary to employ a 110 lbf (489 N) capacity 7 strand cable and to modify the cable connection to ensure that the cable would withstand the loads developed when it was suddenly extracted from the transducer at speeds up to 15 miles per hour (6.71 m/sec).

Two high-speed motion picture cameras were used for photographic coverage of the drop tests. The maximum camera speed was 4000 frames per second and high speed movie film was used to reduce the amount

of auxiliary lighting required. A time base for the film was provided by a lamp enclosed in the camera housing which produced marks along one edge of the developed film outside the picture area. The frequency of the light was controlled so that an interval of 0.00833 seconds occurred between successive flashes.

The basic recording instrumentation consisted of two types of transient waveform recorders which convert analog signals to digital form, store the signal data in a memory and reproduce the original signal when desired. The recorded output is a reconstructed analog facsimile to the input. The memory can be operated so as to freeze its contents, recirculate them and make them available for repetitive readout on an oscilloscope or a chart recorder. Two of the recorders used had two 1024 word memories and one of the recorders had four 1024 word memories which could be operated as a single channel 4096 word memory recorder. Since there was some uncertainty in selecting the sample rate for recording the signals, the procedure used was to record the acceleration and displacement data on several recorders, using different time base selections. A block diagram of the recording instrumentation is shown in Figure 7.

7.3 Measurement Procedure

The simulated bumper was positioned for the drop tests by attaching it to the monorails of the lower hoist on the 12-million-lbf capacity universal testing machine, shown in Figure 2. First a 6 foot (1.83 m) long spreader bar was bolted to the ends of the monorails which extended about 14 feet (4.27 m) from the center of the working space on one side of the testing machine. A solenoid operated quick release having a rated capacity of 4,500 lbf (20.0 kN) was then bolted to the spreader bar. A 2 foot (0.61 m) long spreader bar was bolted to the top of the bumper support structure and the bumper was then attached to the quick release with a shackle bolted to the latter bar. Steel cables were connected from the top of the bumper to the monorails. The cables had enough slack to permit the bumper to fall freely over the desired length and to intrude into the vehicle side, but they constrained the bumper from excessive rotation and from falling to the floor after impacting the vehicle. The elevation of the bumper was controlled by moving the machine sensitive crosshead to which the monorails were attached.

The test vehicle was attached to the support frame in the same manner as for the static tests, and the vehicle-frame assembly was moved into position below the elevated bumper. Prior to anchoring the support frame to the testing machine tie-down floor system, the vehicle was aligned with respect to the bumper using plumb bobs suspended from the bumper in the same manner as for the static test setup. After the support frame was attached to the tie-down floor, arrangements were made for triggering the recording instruments and providing a displacement reference marker for determining the bumper position when analyzing the high-speed movies after completion of the test.

The dynamic test setup, reconstructed after one of the tests, is shown in Figure 8.

The recording instruments were triggered by a microswitch equipped with a nylon cord strung above the test vehicle side structure. As the bumper fell, it deflected the cord so that the microswitch would be activated when the bumper was about 1 inch (2.54 cm) above the vehicle door surface. The signal lead from the microswitch was attached to a triggering circuit which generated a 14 dc-volt decaying pulse of about 12 microseconds duration when the switch was closed. This signal was fed to the triggering inputs of each of the recorders which were adjusted to be activated simultaneously.

A displacement reference marker was provided by attaching alternate light and dark pieces of tape to a channel member which extended through the window opening of the front door of the test vehicle. Sections of this tape were also attached to several of the bumper support tubular members to assist in determining the bumper position when the high-speed movies were analyzed.

Several preliminary drop tests were made on one side of Vehicle "A", which had been tested earlier, in order to determine the proper time base settings for the waveform recorders. Since there was some uncertainty in choosing the time base, the recorders were adjusted for different durations, varying from 20 to 100 milliseconds. The drop heights used for the preliminary tests were about 1 to 2 feet (0.30 to 0.61 m). Vehicle "A" was then removed from the machine and Vehicle "C-1", an untested vehicle, was installed. This vehicle was similar in design and construction as Vehicle "B-1" but was in better condition. The drop height for Vehicle "C-1" was based on the energy absorbed by Vehicle "B-1" during one of the static crush tests. This energy value was computed from the measured force versus deformation data on the door structure. In order to produce the same amount of kinetic energy during the drop test as the energy absorbed for the static test, it was necessary to drop the bumper 7.5 feet (2.29 m) so its impact speed would be 15 miles per hour (6.71 m/sec).

Two high-speed movie cameras were focused so that they would record the striker motion just prior to its impact with the vehicle side structure and the entire bumper motion during subsequent crushing of the structure. An adjustable transformer was employed to reduce the line voltage to obtain a camera speed of about 2000 frames per second. A color movie camera having a speed of about 24 frames per second was used to record the entire drop test. The cameras were started just prior to activating the quick release which dropped the bumper.

8. ANALYSIS OF DATA

8.1 Static Crush Tests

8.1.1 Strain Measurements

Some useful information was obtained from examination of the strain data taken during the static crush tests of Vehicles "A" and "B-1". A summary of those locations in which the largest strains were measured is shown schematically in Figures 9a, 9b and 9c.* The largest strains, indicated by the open circles, were measured along the sill and on the sheet metal supporting the front door hinges for each of these vehicles. Large strains measured on the portion of the B pillar above the window opening on the right side of Vehicle "A" and the left side of Vehicle "B-1" were in a local buckling region of the pillar. The location of this region, which was 2 to 3 inches (5.1 to 7.6 cm) above the lower edge of the window opening, was not known when the left side of Vehicle "A" was loaded. Additional locations where large strains were measured on Vehicle "B-1" are attributed to one or more of the following: 1) the larger magnitude of the applied load, 2) the difference in construction of the frame members for Vehicles "A" and "B-1" and 3) the effect of the door side guard beam which was not present in the door structure of Vehicle "A".

Additional observations may be made from analysis of strain data presented in a graph of load versus strain for a particular location or for adjacent locations on the side structure. An example of the former is shown in Figure 10, which gives the load versus strain measured in the X direction on the sheet metal supporting the upper front door hinge of Vehicle "A" during the crush test of its left side. Even though variations exist in the strain with increasing load, an envelope for this data encompassing the extreme points would be relatively narrow and uniform. This observation suggests that the loading at this position was essentially continuous throughout the test, a suggestion further supported by examination of displacements measured in this region, the data for which will be discussed later. An examination of the load versus deflection measured in this region was made for purposes of a graphical estimation of the load required for buckling of the sheet metal; however, the deflection data were not sufficiently uniform to permit this to be achieved.**

---

*The convention for the coordinate system and the vehicle pillars used in discussion of the measurements is also shown in these figures.

**This may be accomplished if experimental data which tend toward limiting values are sufficiently hyperbolic in character [6].

An example where strain data obtained from gages at adjacent locations may be used to gain insight concerning the sequence of loading of various components is shown in Figure 11, where strains measured at the front and rear door side guard beams of Vehicle "B-1" are compared with the strain at the B pillar in line with the top edge of the door beams. It is observed from this plot that the strain in the side guard beam follows the same trend as that measured on the B pillar up to a crush load of 16,000 lbf (71.2 kN). Thereafter, the strain developed in the B pillar decreases (probably due to the local buckling previously noted), while that in the side guard beam continues to increase.

Relatively little can be concluded from comparison of the strains measured in different directions since the data represent only the localized strain conditions, which may be quite discontinuous. It should be noted, however, that large strains were measured in all directions on the sheet metal adjacent to the front door hinges and along the sill. This result is in apparent agreement with a conclusion by Dale, et al, that the supporting sheet metal structure of latches and hinges usually fails before the latches or hinges [7].

The principal usefulness for strain measurements in this investigation was to obtain qualitative and comparative information about vehicle side structure crush characteristics. Useful insights can also be gained regarding the load transmission during a static crush test, as shown by the above examples, to supplement interpretation of measured displacements during these tests.

8.1.2 Analysis of Static Displacements

The positions on the side structure at which displacements were measured for the vehicles were the front and rear doors, the A and B pillars and the displacement between the pillars. In addition, displacements were measured at a door side guard beam and the front seat for Vehicle "B-1", and the firewall for both vehicles. The front seat and firewall, although internal structural members, may be considered as part of the side structure in the sense that they sustain loads during crushing of the vehicle side. For convenience in distinguishing between various structural degrees of freedom for the vehicle components, the test results are analyzed in terms of the following modes of deformation 1) doors, side guard beam and B pillar lateral deformation, 2) A and C pillars and additional modes of B pillar deformation, 3) deformation of internal structural members, and 4) local failure of structural members, joints and connections.

8.1.2.1 Doors, Side Guard Beam and B Pillar Lateral Deformation

The doors and B pillar are considered together because it was observed that they tended to deform as a unit in resisting lateral intrusion, especially in the early portion of the static crush tests. The displacement of the B pillar was measured at two positions located

at the same elevation (Y direction), one being located forward and the other rearward of the center of the pillar. This was done to discriminate between the translational intrusion deformation (parallel to the Z axis) and rotational deformation of the pillar (in the X-Z plane) which is described in the following section. The load versus intrusion deformation measured at several locations during crush tests of the Vehicle "A" left and right sides and the Vehicle "B-1" left side are shown in Figures 12, 13, and 14, respectively. The location of the displacement transducers on the doors and B pillar for Vehicle "A" was about 14 inches (35.6 cm) above the rear floorpan. The corresponding position on Vehicle "B-1" was about 17 inches (43.2 cm) above the door base and the displacement transducer attached to the rear door side guard beam was about 14 inches (35.6 cm) above the base of the door near the center of the beam. The vertical positions of all these transducers were approximately in line with the center of the simulated bumper. An example of the structural response of a component over the entire loading and unloading cycle is shown in Figure 15, for a side guard beam of Vehicle "B-1".*

One general observation from the measured intrusions is that the B pillar deformation was always less than that measured at the doors. This result is to be expected since the door outer panels, to which the end of the transducers were attached inside the doors, began to deform before significant loads developed through the front door latch and rear door hinges to the B pillar. Another observation is that the deformation measured at the front door was generally larger than at the rear door.** At the conclusion of the test, the edge of the front door adjacent to the B pillar was observed to have intruded further than the corresponding edge of the rear door. The portion of the rear door nearest the latch appeared to have rotated about the latch as the door was crushed, probably due to the striker curvature in this region. A plot of the maximum intrusion profile for the right side structure of Vehicle "A" is shown in Figure 16.

Lateral deformation of the B pillar was determined by taking an average of the deformations measured at two points at the same elevation spaced about 12 inches (30.5 cm) apart. The cables of the transducers were attached to a stiff plate which was bolted to the B pillar to accomplish this measurement. By examination of the data obtained from each transducer, the load range over which the B pillar exhibited uniform lateral deformation could be determined. For Vehicle "A", this region extended to a crush load of about 11,000 lbf (48.9 kN), beyond which the deformation became more complex. Thus the data

---

*The elastic recovery observed from analysis of the data at this location was about 0.8 inch (2.03 cm).

**This result was achieved only during the static crush tests, during which the simulated bumper was constrained to move in one direction.

for the B pillar deformation plotted in Figures 12 and 13 were limited to this range. For Vehicle "B-1", the lateral deformation of the B pillar tended to be more uniform over the entire load range.

It should be noted that there were differences in both the design and the deformation modes for the B pillars of Vehicles "A" and "B-1" which could influence the pillar response. The sheet metal thickness for the B pillars of Vehicle "A" was 0.055 inch (1.40 mm), whereas the corresponding thickness for Vehicle "B-1" was 0.080 inch (2.03 mm). In addition, the distance between the B pillar and the front seat for Vehicle "A" was about 3 inches (7.62 cm), whereas the corresponding distance for Vehicle "B-1" was about 3.5 inches (8.89 cm). It is not known precisely when the B pillars first came into solid contact with the front seat, but based on visual observations made during the test this occurred at a load of about 12,000 lbf (53.4 kN) for Vehicle "A" and at about 23,000 lbf (102.3 kN) for Vehicle "B-1". Plots of the maximum intrusion profile of the B pillar for Vehicles "A" and "B-1" are shown schematically in Figures 17 and 18, respectively.

8.1.2.2 Deformation of A and C Pillars and Additional B Pillar Modes

Plots of the deformation measured at the A pillar versus load for the Vehicle "A" right side and Vehicle "B-1" left side are shown in Figure 19. The end of the transducer cable was located near the lower hinge, about 6.5 inches (16.5 cm) above the floorboard, for Vehicle "A" and midway between the hinges, about 12 inches (30.5 cm) above the floorboard, for Vehicle "B-1". It is observed that the deformation increased uniformly with load at this location. Visual examination of the sheet metal around the front door hinges indicated that the A pillars experienced significant rotational, as well as translational, deformation. This result is attributed to the design of the simulated bumper whose curved front surface would tend to induce rotation of the A pillar against which the curved portion was bearing.

Another mode of deformation is indicated by a measurement of the change in the distance between the A and B pillars during the crush test of the Vehicle "A" left side, plotted in Figure 20. The displacement transducer used for this measurement was located in a horizontal position (parallel to the X axis) about 12 inches (30.5 cm) above the floorboard. Similar measurements were made of the change in the distance between the B and C pillars for the right side of Vehicle "A" and the left side of Vehicle "B-1", as shown in Figures 21 and 22, respectively. For Vehicle "A", the distance between the B and C pillars first increased and then decreased up to a load of about 18,000 lbf (80.1 kN). Beyond this load, the distance between the pillars increased continuously for the remainder of the test. For Vehicle "B-1", the distance between the B and C pillars decreased a small amount up to a load of about 4,000 lbf (17.8 kN). Thereafter, the distance between the pillars increased continuously until a load

of about 24,000 lbf (106.7 kN), after which the range of the transducer was exceeded. At the conclusion of the test of Vehicle "B-1" it was found that the A and C pillars were about 0.5 inch (1.27 cm) closer together than their original separation.

No measurements were made of the C pillar deformation other than its deflection relative to the B pillar. Strain data recorded at several locations on the sheet metal adjacent to the rear door latch indicated that significant strains never developed in this region. There was no visible deformation of the C pillar during the test on the Vehicle "A" left side. For the test on the Vehicle "A" right side, there was a region of local buckling near the roof structure and at the rear window opening in the vicinity of the C pillar. After the test on Vehicle "B-1", the only observed deflection of the C pillar was some small deformation of the sheet metal near the top of the rear seat. A vertical profile showing the relative permanent deformation of the three pillars after the crush test of Vehicle "B-1" is shown schematically in Figure 23.

The angular deformation of the B pillar (in the X-Z plane), which was derived from analysis of the two displacement measurements previously noted, for the right side of Vehicle "A" and the left side of Vehicle "B-1", is plotted in Figure 24. This deformation was determined by taking the difference in the displacements measured at two locations on a stiff plate bolted to the pillar for each recorded load, dividing this difference by the distance between the transducer positions and converting the resulting value to an angle. This deformation was determined by taking the difference in the displacements measured at two locations on the pillar for each recorded load, dividing by the distance between the transducer positions and converting to an angle.

In summary, the measured deflections show that significant deformations of the B pillar for Vehicles "A" and "B-1" include lateral displacement (parallel to Z axis), longitudinal displacement (parallel to X axis), angular displacement (in the X-Z plane) or some complex combination of these responses at various loads throughout the tests. A relatively small number of positions were selected for the measurements of each of the principal structural components in order to include as many components as possible. The local buckling, yielding and fracturing of components observed after the tests, which will be reviewed later, provided additional insight for a more complete evaluation of member performance during the static crush tests.

8.1.2.3 Deformation of Internal Structural Members

The deformation of the firewall was measured at one location, parallel to the X direction, during the crush tests for the Vehicle "A" right side and Vehicle "B-1" left side. This data is shown plotted in Figure 25. The firewall surface contour of both vehicles was quite nonuniform and the deformed profile after the tests was complex. In order to highlight the topography of the deformed firewall surface, a 2 inch (5.08 cm) square grid was painted on the firewall before

the test for Vehicle "B-1". Photographs taken before and after the crush tests are shown in Figure 26. For complex components such as the firewall, such a grid can be used to supplement deflection measurements and to indicate appropriate positions for the transducers if additional displacement measurements on similar vehicles are desired.

Since it was expected that the front seat of the vehicles would afford some resistance to intrusion into the occupant compartment, an attempt was made to measure the deformation of the seat at one location. During the crush test of the Vehicle "B-1" left side, the end of a cable transducer was attached to the structural member at the top of the front seat at its midspan. The recorded deformations in the longitudinal (X) direction versus the crush load are plotted in Figure 27. This result shows that the seat exhibited considerable deformation at loads above 23,000 lbf (102.3 kN). The maximum deformation at the midspan of the seat exceeded the range of the transducer after a load of about 28,000 lbf (124.5 kN). A useful method for determining the effectiveness of a front seat in resisting a side crush load would be to crush two identical vehicles, one having the seat and the other without, and compare the load versus deflection of the side structural members for the two tests.

8.1.2.4 Local Failure Modes of Structural Members, Joints and Connections

The modes of failure for components other than those established from the measured deflections and for structural connections included local buckling, yielding in a localized plastic zone or combinations of buckling and plastic yielding, and fracture.

During the crush test of the Vehicle "A" left side, the first observed regions of local deformation other than the doors were on the sill adjacent to the B pillar and at the junction of the forward end of the sill with the vehicle front quarter panel. These regions, which are shown encircled in Figure 28, appear to indicate that the initial small crush loads were transferred through the doors and A and B pillars to the sill.* Other regions encircled on the B pillar in this photograph reveal an angular deformation at the surface of the sheet metal supporting the rear door lower hinge and a complex region of local buckling and yielding on the B pillar several inches above the door window sill. After the test, it was observed that the sheet metal between several of the spot welds in this region of the pillar had buckled and the sheet metal had torn away from one of the welds.

---

*The doors were removed from the vehicle for this photograph in order to highlight the deformation of the pillars and sill.

As can be observed from Figure 28, the central portion of the B pillar appears to have been displaced uniformly toward the occupant compartment, which is further indicated by the small strains recorded in this region. The above noted zone of yielding occurred in the upper portion of the pillar just above where the reduced cross section of the pillar began. A similar failure mode occurred during the test of the Vehicle "A" right side in the same region, but less buckling developed in the sheet metal between adjacent spot welds. This localized deformation was probably related to the previously described changes in displacement measured between the pillars.

During the crush test of the Vehicle "A" right side, a maximum load of 20,000 lbf (89.0 kN) was applied. After the test it was observed that the spot welds at the base of the B pillar had fractured. A photograph showing this region on the inboard side of the pillar is given in Figure 29. Sheet metal fractures were also observed at several spot welds which joined the outer surface of the B pillar to the sill, and at two diagonal corners of the rear window opening.

Considerable buckling occurred across the dash during the test of the Vehicle "A" right side, as shown in Figure 30. Since no significant deformation of the dash was observed for loads up to 15,000 lbf (66.7 kN), the dash buckling developed somewhere between this load and the maximum applied load of 20,000 lbf (89.0 kN). The deformation which initially occurred in the middle of the dash precipitated a fracture at the base of the windshield adjacent to the dash, and the large deformations which occurred later caused fracture of the front glass adjacent to the A pillar.

During the crush test of the Vehicle "B-1" left side, a major fracture developed in the B pillar where the pillar cross section changed shape just above the door window sill. The deformed profile of the B pillar at the conclusion of this test, shown schematically in Figure 18, suggests that a zone of plastic yielding could have formed in this region which led to the fracture of the pillar.

The displacement of the B pillar near the roof was measured during the test of the Vehicle "A" right side. Its deformation with respect to the B pillar on the left side of the vehicle is shown in Figure 31, for a portion of the load range. The strains at the intersection of the B pillar and roof structure were generally small and no fractures occurred in this region except at the larger crush loads during the last portion of the test of Vehicle "B-1". There was some local yielding and separation occurred between the roof cross beam and the roof sheet metal near the B pillar for each of the tests. This deformation was apparently related to the local buckling of the roof sheet metal adjacent to the pillar which was observed during the tests.

The crush test on the left side of Vehicle "B-1" was more severe than the tests of Vehicle "A". Sheet metal fractures were generated in the sill near the B pillar, at the base of the A and B pillars

and at the top of the A pillar near the roof, and there was local buckling along the top edge of the front window frame during the test of Vehicle "B-1". The strain which was determined at one location on the front glass was insignificant. No fractures developed anywhere on the front glass during the test until loads of 20,000 lbf (89.0 kN) or larger were applied, after which a fracture developed near the A pillar and the front glass began to separate from its molding around the top and sides of the window opening. Fractures which developed in the sheet metal at several corners of the rear window opening of Vehicle "A", whose rear window had been removed, were not observed during the test of Vehicle "B-1" whose rear window was left installed.

As a final example of a localized failure mode, the deformation of the side guard beam for the rear door of Vehicle "B-1" is considered. Examination of Figure 15 indicates that the response of the side guard beam could be approximated by a series of several successive increments over which the measured load versus deformation is approximately linear. The nature of this response resembles that of a built-in beam, loaded by a concentrated force, which experiences several piecewise linear load versus deflection increments due to the formation of plastic hinges before final collapse [8, 9]. An examination of the deformed rear door after the test of Vehicle "B-1" indicates that it did experience a load which was distributed over a small area near its midspan due to the relative position of the door with respect to the curved portion of the simulated bumper. Figure 32 shows the deformation of the rear side guard beam which was photographed after removing the outer panel of the rear door. A more detailed investigation would be required in order to determine whether the failure of the side guard beams in fact develops due to successive formation of plastic hinges.

8.2 Dynamic Crush Tests

For the drop test on Vehicle "C-1", the simulated bumper intruded into the vehicle side structure about 13 inches (33.0 cm) and then rebounded several inches before rotating and sliding away from the door toward the roof structure. Subsequent analysis of the high-speed movies indicated that the top edge of the bumper moved about 19 inches (48.3 cm) with respect to the displacement reference marker, the last 6 inches (15.2 cm) of which was associated with rotational motion and sliding of the bumper. One of the two constraining cables broke after the bumper began rotating in the direction of the roof structure, after which the bumper impacted the front of the roof and the hood before coming to rest. The movies indicated that some local buckling of the roof structure had occurred prior to breaking of the cable. A plot of the bumper displacement with respect to the fixed reference marker versus time is shown in Figure 33. The maximum deceleration

recorded at the center of the bumper was about 7 g.*

Vehicle "C-1" was removed from the testing machine and Vehicle "B-2", which was identical to Vehicle "B-1", was installed. The vehicle was oriented so that the falling bumper would strike it in the same position as during the static test on Vehicle "B-1". The drop test was conducted in the same manner as for Vehicle "C-1" with the same drop height. For this test, modifications were made to strengthen the cable and to reduce the effect of the sharp edges of the testing machine monorails which were believed to contribute to breaking the cable during the previous test. These modifications proved successful in constraining the bumper after its maximum intrusion into the vehicle side structure.

The bumper displacement with respect to the fixed reference marker versus time was determined from analysis of a high-speed movie, and was found to correspond closely to similar data obtained from the test on Vehicle "C-1" for displacements up to 16 inches (40.6 cm). The values of displacement versus time obtained from the movies by two observers generally agreed within about 5 percent. The maximum deceleration recorded at the center of the bumper was about 6 g.

The output signals from the displacement transducers attached to the front and rear door side guard beams were oscillatory in form and were not well defined. It is believed that stress waves in the transducer cable or in the member connecting the transducer to the door beam were recorded. The structural components generally deform in several directions during vehicle crushing, as the static test data indicated, further complicating analysis of the signals.

In order to determine the deformation of the door structure at various time intervals during the impact, polynomial equations of various orders were fitted through the data points obtained from analysis of the movie film. It was found that several polynonial equations gave essentially the same curve which passed through the experimental data. An attempt to differentiate these equations to obtain acceleration versus time information from the measured displacement versus time data proved unsuccessful, since several distinct solutions seemed to be plausible. The displacement versus time information was useful, however, in correlating the bumper acceleration and deformation of the front door panel at different time intervals. The bumper accelerations were converted to force, using the known mass of the bumper. The resulting transient load versus deformation data for the dynamic tests is compared with the static test results in the following section.

---

*Acceleration values are frequently given in terms of "g", the acceleration due to gravity (9.80665 m/s).

9. COMPARISON OF STATIC AND DYNAMIC TEST RESULTS

Several methods can be employed to compare the static and dynamic crush test results. Figure 34 shows the overall damage incurred in the side door structure during the static test of Vehicle "B-1" and the dynamic test of Vehicle "B-2". A plot of the exterior deformation of the vehicle left side after the two tests is shown in Figure 35. An examination of the permanently deformed rear door side guard beam after the drop test for Vehicle "B-2" is shown in Figure 36, which can be compared with the corresponding damage produced during the static crush test of Vehicle "B-1" which was shown in Figure 32.

In order to compare the transient load applied to the Vehicle "B-2" door structure during the dynamic crush test with the static load applied to the side of Vehicle "B-1", the deformation of the front door panel at various time intervals was first obtained from the movies taken during the drop test. The values of door panel deformation were then plotted with respect to the transient load obtained from analysis of the acceleration signals measured at the center of the bumper at corresponding increments of time, starting when the door was first deformed. This data is presented in Table 2 and is also plotted in Figure 37. The acceleration data used to compute the dynamic load represents the maximum single amplitude of the basic signal which was recorded, ignoring both low frequency electrical noise and high frequency spurious noise components.

The ratio of the static to dynamic loads at corresponding values of the door panel deformation can be interpreted as dynamic empirical factors for comparing the static and dynamic crush characteristics of the door structure. It should be noted that the sudden decrease in the dynamic load value after a door deformation of about 5.4 inches (13.7 cm) is probably due to some change in the distributed load across the face of the simulated bumper. Examination of the deformed side doors following either static or dynamic crush tests has indicated that toward the end of the test, the largest forces tend to be applied away from the bumper center and near the curved portions of its face.

The applied loads for the two tests were compared for only a limited range of door panel deformation. As shown in the series of movie frames of the drop test immediately after the bumper impacted the side of Vehicle "B-2", there is a tendency for the bumper to rotate toward the rear door initially and afterwards to rotate in another plane, toward the roof structure. Thus, one interpretation for the sudden decrease in the acceleration measured at the center of the bumper is that it may represent the onset of rotational motion of the bumper after its linear motion has essentially terminated. The load factors in Table 2 obviously are most meaningful when the motion of the bumper is principally in one direction, as during the static tests.

Comparison of the damaged Vehicle "B-2" after the drop test revealed that its B pillar had experienced local plastic yielding near its midpoint at the lower level of the door window opening. In addition, the B pillar had been crushed against the front seat as the B pillar had been during the static crush test of Vehicle "B-1". The lesser amount of damage done to the seat and the dash of Vehicle "B-2" for the drop test than during the corresponding static test of Vehicle "B-1" is believed to be due to the smaller range of linear striker motion during the drop test than for the static test. Measurements taken before and after the drop test indicated that the permanent deformation of the front and rear door side guard beams for Vehicle "B-2" was about 6.45 inches (16.4 cm) and 7.50 inches (19.0 cm), respectively.

From an examination of the permanently deformed door structures of Vehicles "B-1" and "B-2", together with the quantitative data presented, it is apparent that the motion of the simulated bumper was significantly constrained during the static crush test. As a consequence of this constrained motion, the forces were applied more uniformly to the front and rear door structures than during the dynamic crush tests as shown by comparison of the deformed structures in Figure 35. In addition, the bumper continued crushing Vehicle "B-1" until the indicated static load had begun to decrease.* The large deformations which occurred in the front seat, dash and firewall during the static crush test were the consequence of the constrained bumper motion. During the drop tests, the bumper linear motion was evidently transformed into rotational motion toward the rear door structure after sufficiently large reactions developed at the forward end of the bumper by the front door and its adjacent frame members. After this motion had developed and the maximum intrusion of the bumper into the door structure had occurred, the remaining inertial forces were expended in the rotation of the bumper toward the roof structure.

10. CONCLUSIONS AND RECOMMENDATIONS

Laboratory test procedures were developed for evaluating the crush characteristics of automotive structural components which perform a major structural function in side impacts. Strain measurements taken during the static tests were useful in determining regions on the back-up pillar and frame members for the door structure where significant strains developed. The load versus deformation relationships of various structural components and the deformations measured between some of the components are a useful method for describing the crush characteristics of vehicle members. Visual examination of permanently

---

*In order to establish guidelines for the maximum static loads to apply to a vehicle, static and dynamic crush tests would have to be conducted and their results correlated for additional vehicles.

deformed members together with some of the measured displacements can be used to determine regions of localized plastic deformation and the significant structural degrees of freedom. The techniques which were developed could be used to determine the crush characteristics of additional structural members and to determine modes of deformation other than those examined in this program. In addition, significant information about the crush characteristics of structural components when loaded at different angles could be obtained with minor modifications to the procedures employed in this program.

The determination of the deformation of vehicle components at loading rates experienced during typical impact speeds requires further development to supplement such generally employed methods as high-speed photography. Techniques for direct measurement of component deformations in several directions at various loading rates places severe requirements on both the ruggedness and accuracy of transducers. In addition, instrumentation costs for dynamic testing tend to become considerably larger than for static testing when detailed information is sought for a large number of members. Although the instrumentation employed for this purpose in this study survived the severe test environment, additional research would be required to minimize wave effects and to ensure that complex motions can be properly measured. The test procedure could be readily modified so the motion of the simulated bumper during the static and dynamic crush tests would more nearly correspond to one another. Furthermore, the photographic techniques could also be refined so that greater resolution of the bumper motion during dynamic tests could be obtained from analysis of high-speed movie films.

The results of this program indicate that static crush data can be very useful in supplementing dynamic laboratory evaluations of vehicle crush characteristics. The test procedures developed may be employed in the evaluation of component designs for limiting intrusion or redistributing loads or to provide techniques for obtaining data required for computer simulations of vehicles during side impacts.

11. ACKNOWLEDGEMENTS

Useful information was provided by B. Krauss and G. Braimmeier who were Contract Technical Managers for this project for the National Highway Traffic Safety Administration. The valuable assistance of A. F. Kirstein, C. Federman, R. S. Koyanagi and R. A. Mitchell in various aspects of this program is gratefully acknowledged. The author is indebted to J. R. Hazzard for design and test assistance, to J. L. Michalak and R. E. Snyder for instrumentation, to N. Halsey for photographic results and to R. W. Peterson for assistance in data reduction.

12. REFERENCES

1. Thompson, J. E., Control of Structural Collapse in Automotive Side Impact Collisions, PhD Dissertation, University of Detroit, 1972.

2. Galganski, R. A., and Napierski, V. F., Basic Research in Crashworthiness II - Development of Moving Barrier Test Technique, Calspan Corp. Report No. YB-2987-V-13, Interim Technical Report to U.S. Dept. of Transportation, National Highway Traffic Safety Administration, Contract No. FH-11-7622, January 1973.

3. SAE Recommended Practice J972a - Moving Barrier Collision Tests, SAE Handbook, Part 2, 1974.

4. Kirstein, A. F., Universal Testing Machine of 12-Million-lbf Capacity at the National Bureau of Standards, NBS Special Publication 355, September, 1971.

5. SAE Recommended Practice J367-Passenger Car Door System Crush Test Procedure, SAE Handbook, Part 2, 1974.

6. Kirstein, A. F., The Hyperbolic Character of Certain Experimental Results Which Tend Toward Limiting Values, NBS Technical Note 435, November 1967.

7. Dale, E. S., et al, Test Procedures and Requirements for Door System Evaluation, Dayton T. Brown, Inc. Final Report No. DTB22P70-1540 for DOT National Highway Traffic Safety Administration under Contract No. DOT-HS-005-1-005, March 1971.

8. Plastic Design in Steel, A Guide and Commentary, ASCE Manuals and Reports on Engineering Practice - No. 41, 1971.

9. Rogers, G. L., Dynamics of Framed Structures, John Wiley and Sons, Inc., 1959.

Table 1 - General Characteristics of the Test Vehicles

Vehicle Designation	Year	Approximate Mileage	Door Side Guard Beam	Side Tested	Type of Test
"A"	1970	82,000	No	Left	Static
			No	Right	Static
"B-1"	1969	200,000	Yes	Left	Static
"B-2"	1969	200,000	Yes	Left	Dynamic
"C-1"	1971	90,000	Yes	Left	Dynamic

Table 2 - Comparison of Applied Loads During Static and Dynamic Crush Tests at Corresponding Values of Side Door Deformation

Front Door Panel Deformation	Static Load[1]	Dynamic Load[2]	Ratio of Static to Dynamic Load
in(cm)	lbf(kN)	lbf(kN)	
1.9 (4.83)	13,100 (58.27)	11,600 (51.60)	1.13
2.8 (7.11)	18,000 (80.06)	17,200 (76.51)	1.05
3.9 (9.91)	22,100 (98.30)	20,900 (92.96)	1.06
5.4 (13.7)	23,800 (105.9)	25,300 (112.5)	0.94
6.5 (16.5)	25,300 (112.5)	17,900 (79.62)	1.41
7.8 (19.8)	27,600 (122.8)	16,400 (72.95)	1.68
9.1 (23.1)	29,100 (129.4)	14,500 (64.50)	2.01

[1]Load during static crush test of Vehicle "B-1" left side.

[2]Load during dynamic crush test of Vehicle "B-2" left side (obtained using acceleration measured at center of simulated bumper and bumper mass).

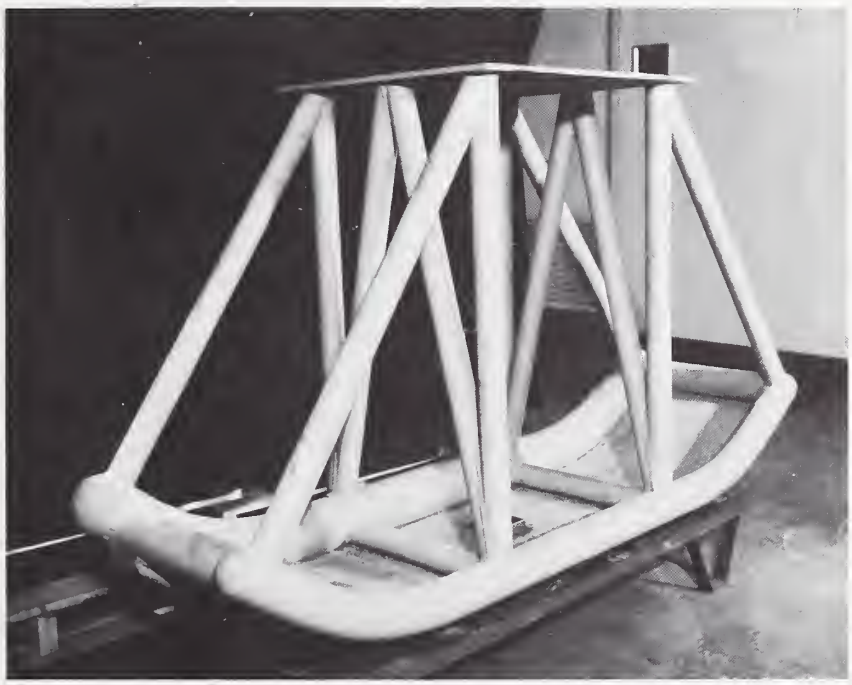

Figure 1 – SIMULATED BUMPER USED FOR STATIC CRUSH TESTS

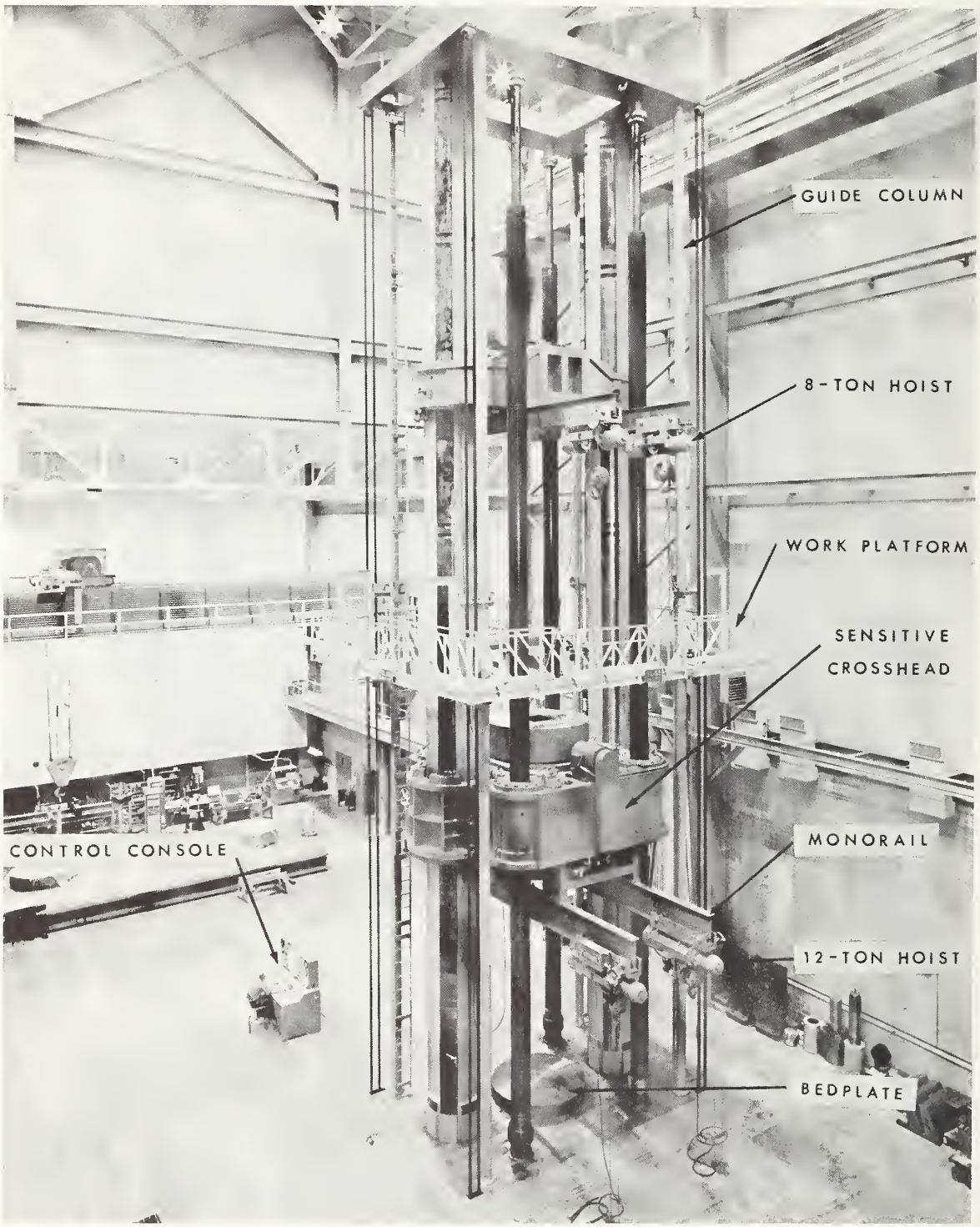

Figure - 2 - UNIVERSAL TESTING MACHINE OF 12,000,000 lbf CAPACITY

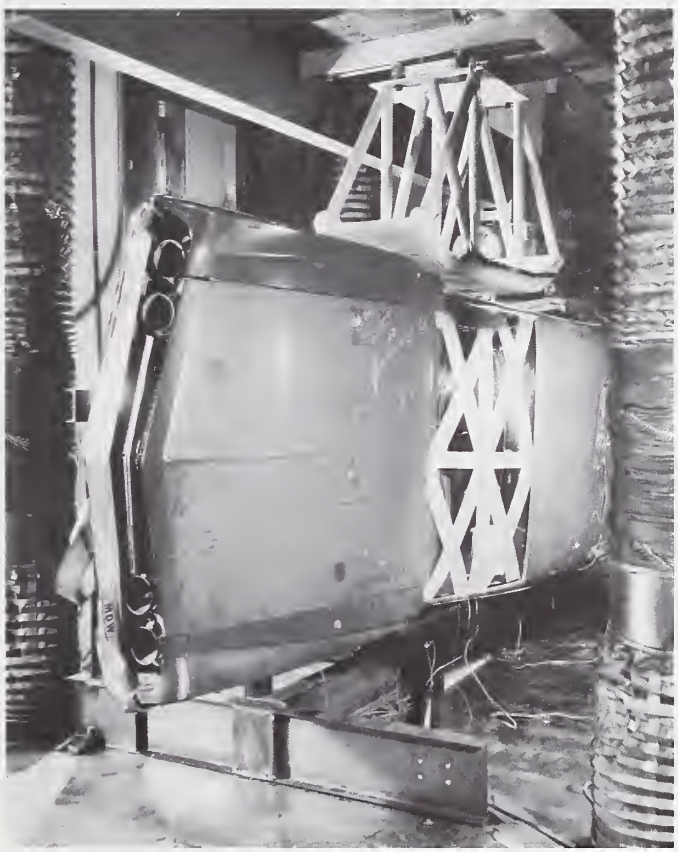

Figure 3 – STATIC TEST SETUP IN UNIVERSAL TESTING MACHINE

Figure 4 - RELATIVE POSITION OF BUMPER AND SIDE STRUCTURE FOR TWO SIMILAR VEHICLES

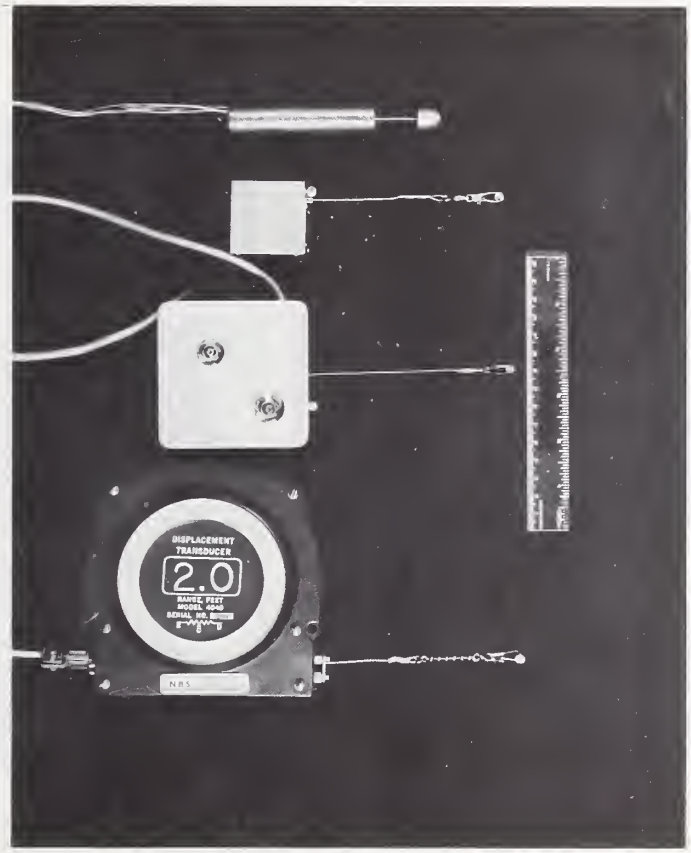

Figure 5 - DISPLACEMENT TRANSDUCERS USED DURING STATIC CRUSH TESTS

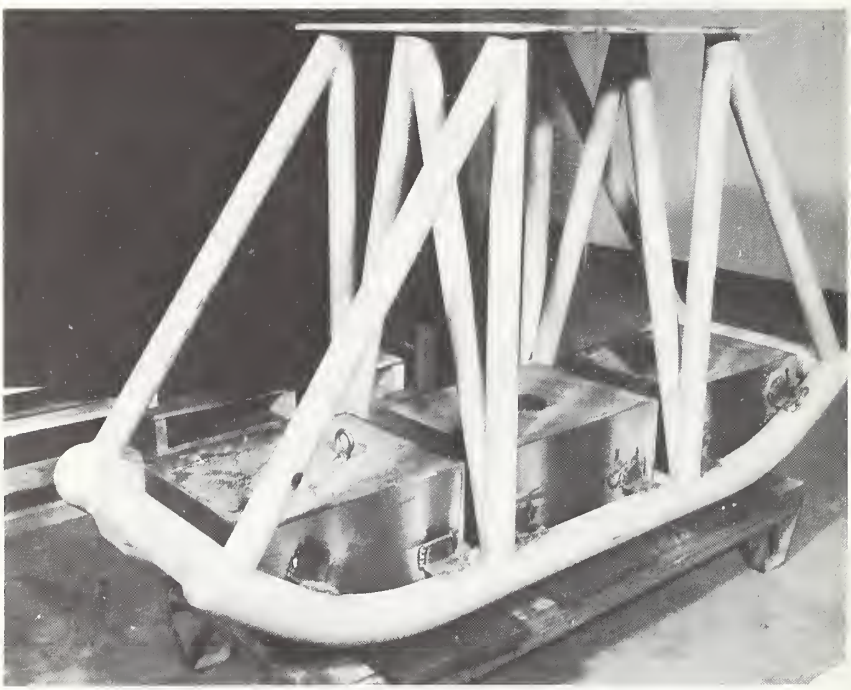

Figure 6 – MODIFIED SIMULATED BUMPER USED FOR DYNAMIC CRUSH TESTS

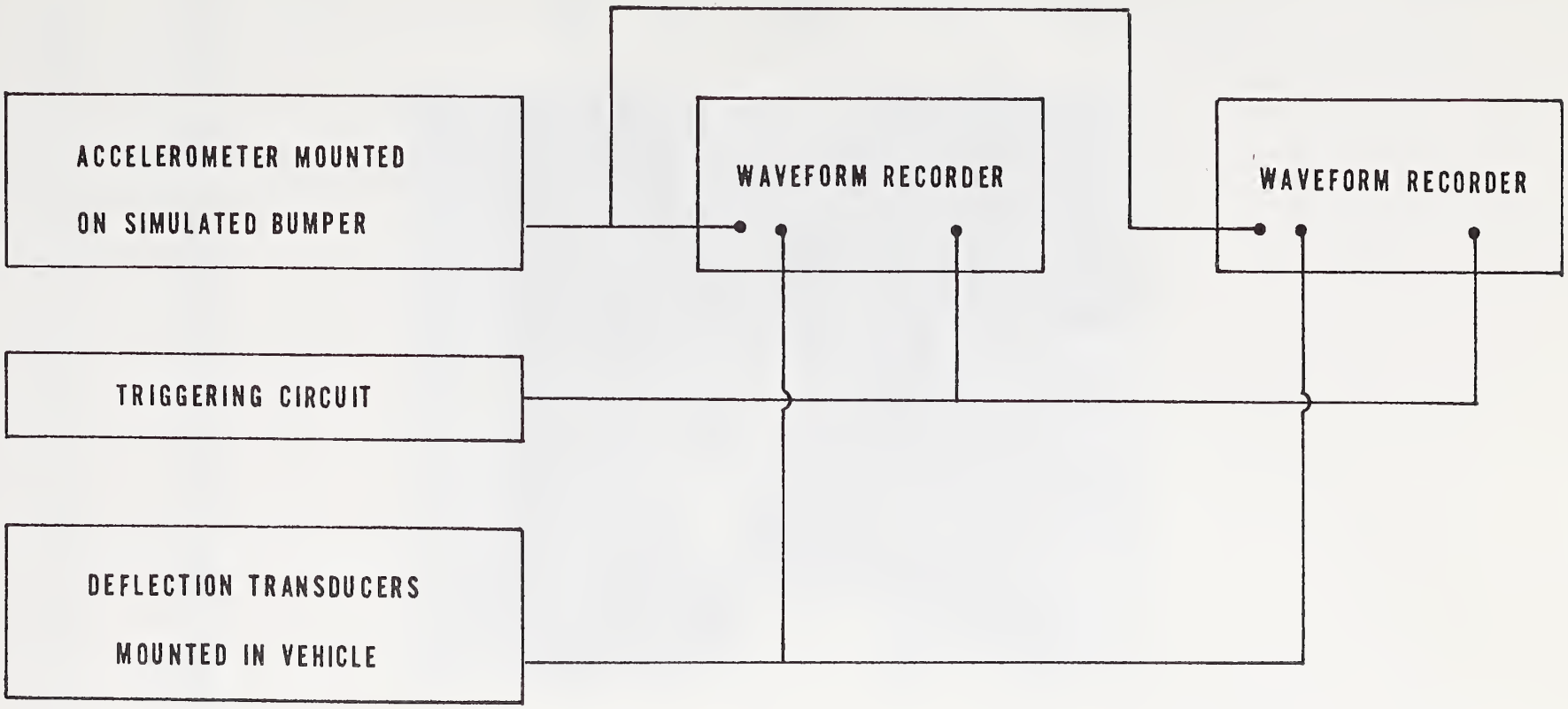

Figure 7– BLOCK DIAGRAM OF INSTRUMENTATION FOR DYNAMIC CRUSH TESTS

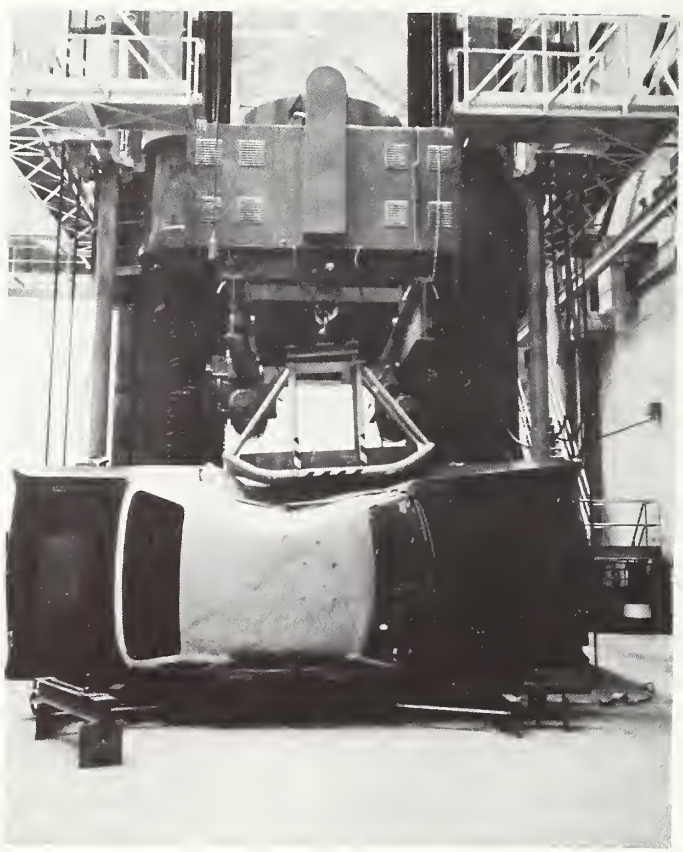

Figure 8 – DYNAMIC TEST SETUP (RECONSTRUCTED AFTER DROP TEST)

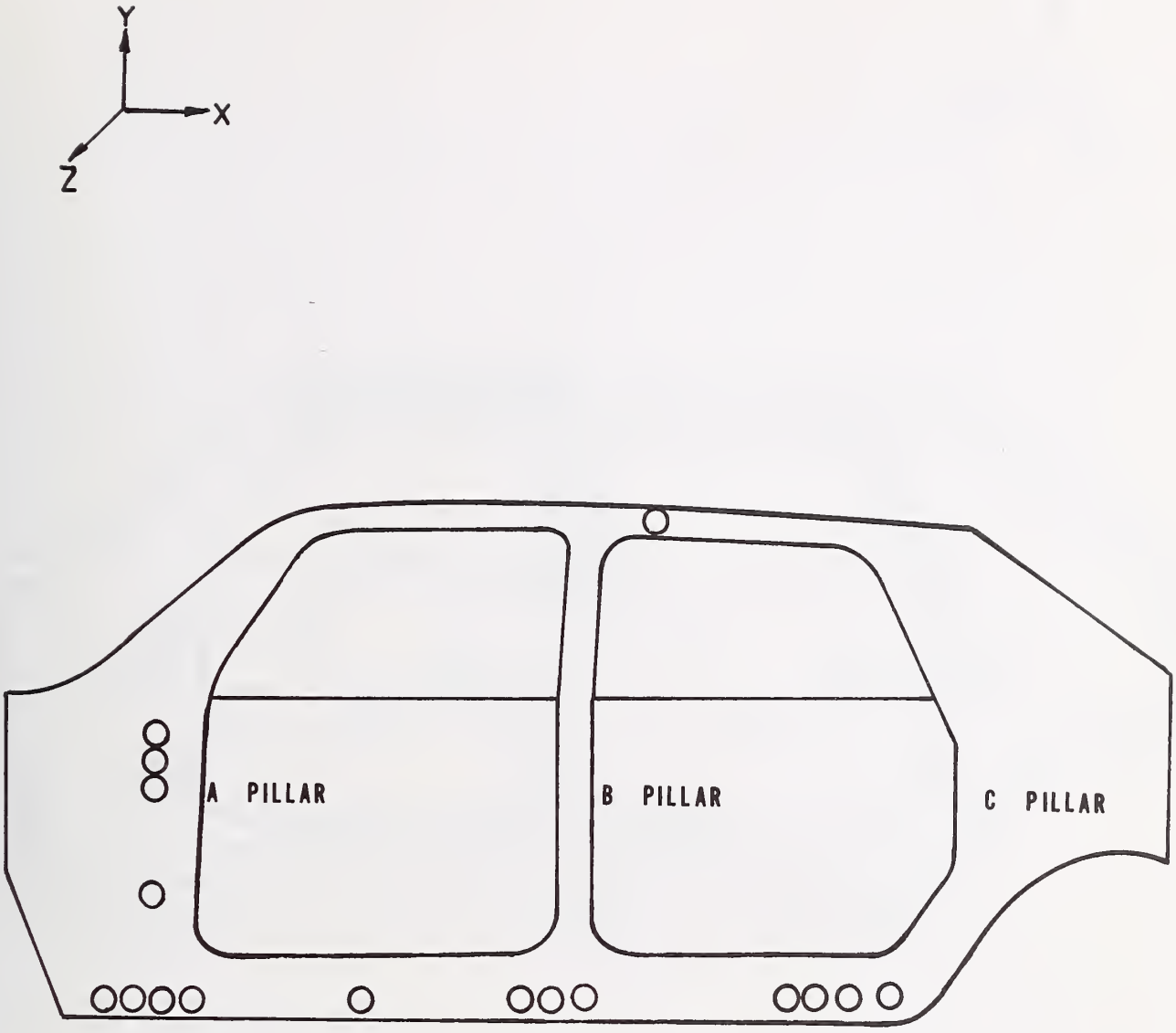

Figure 9a – SCHEMATIC OF VEHICLE A LEFT SIDE SHOWING REGIONS OF MAXIMUM RECORDED STRAIN

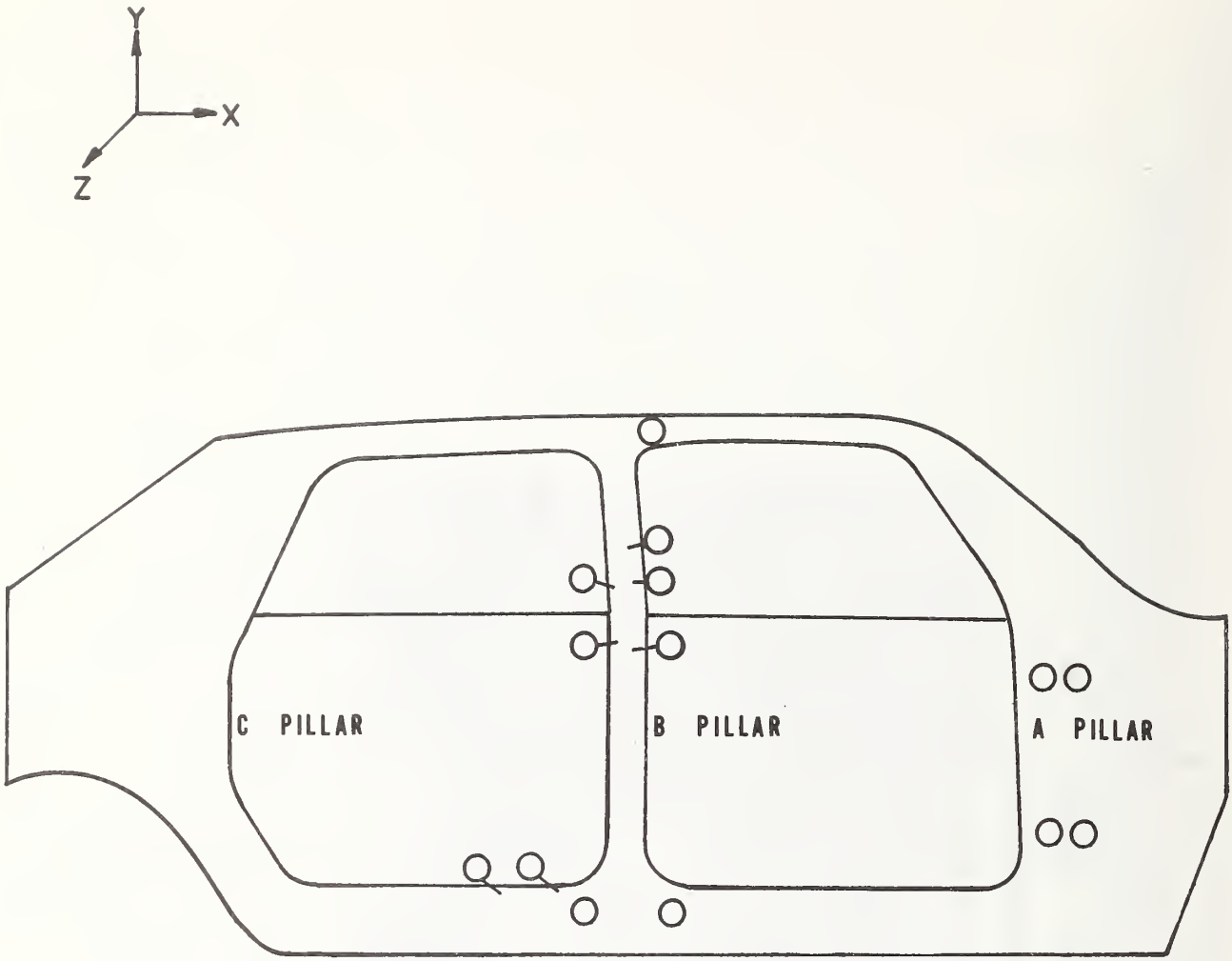

Figure 9b – SCHEMATIC OF VEHICLE A RIGHT SIDE SHOWING REGIONS OF MAXIMUM RECORDED STRAIN

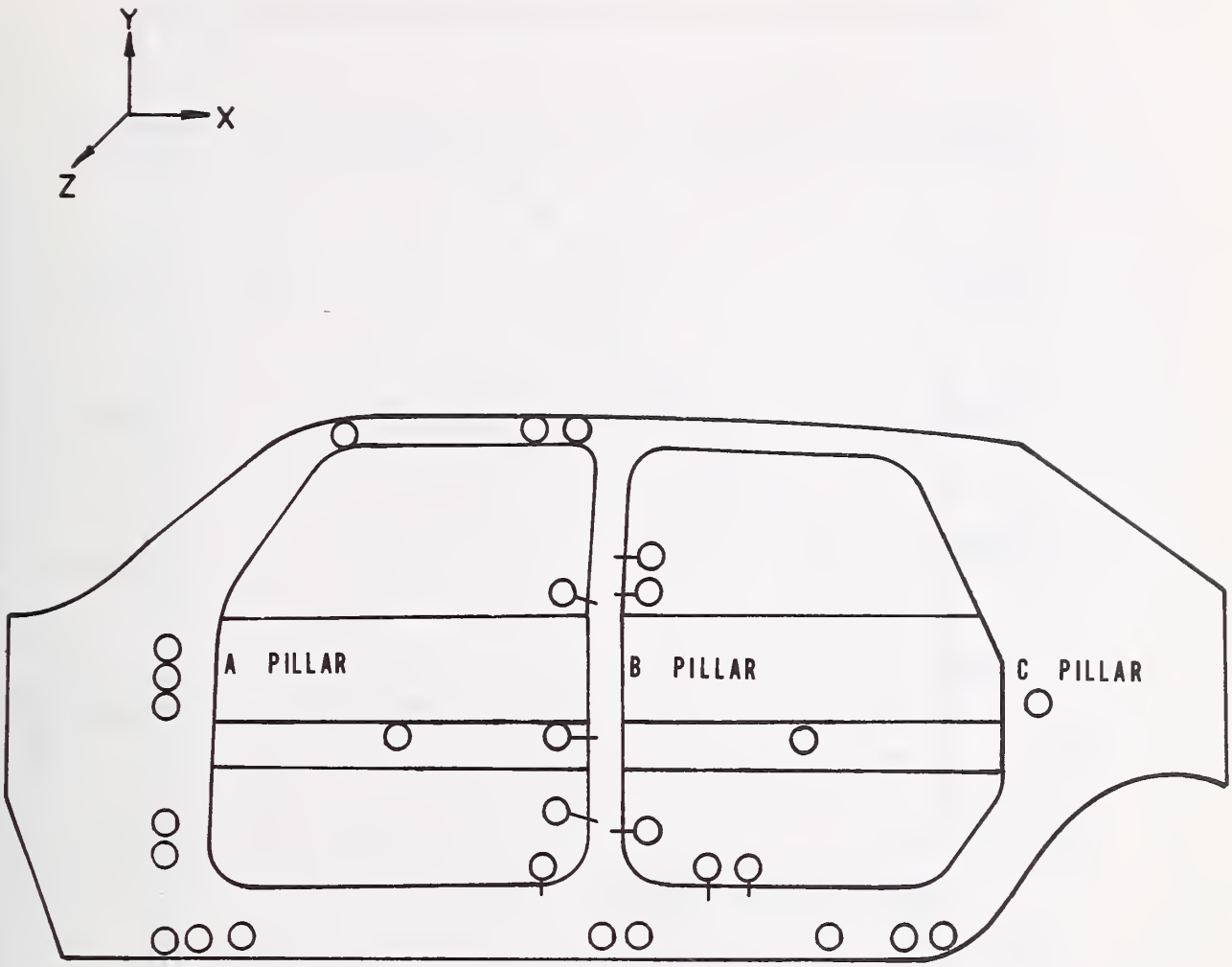

Figure 9c – SCHEMATIC OF VEHICLE B–1 LEFT SIDE SHOWING REGIONS OF MAXIMUM RECORDED STRAIN

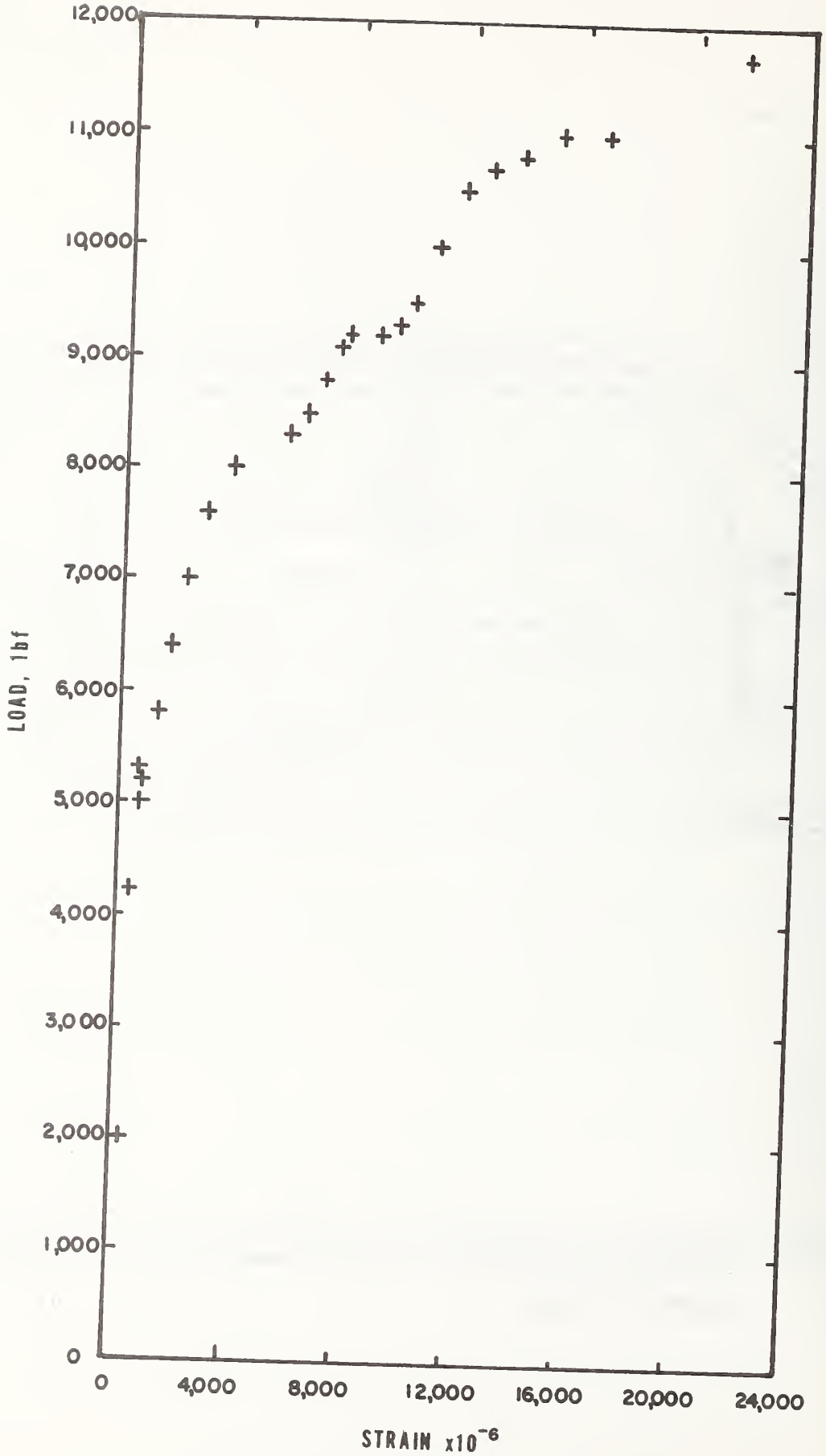

Figure 10 — LOAD VERSUS STRAIN AT A POSITION ON THE A PILLAR OF VEHICLE A LEFT SIDE

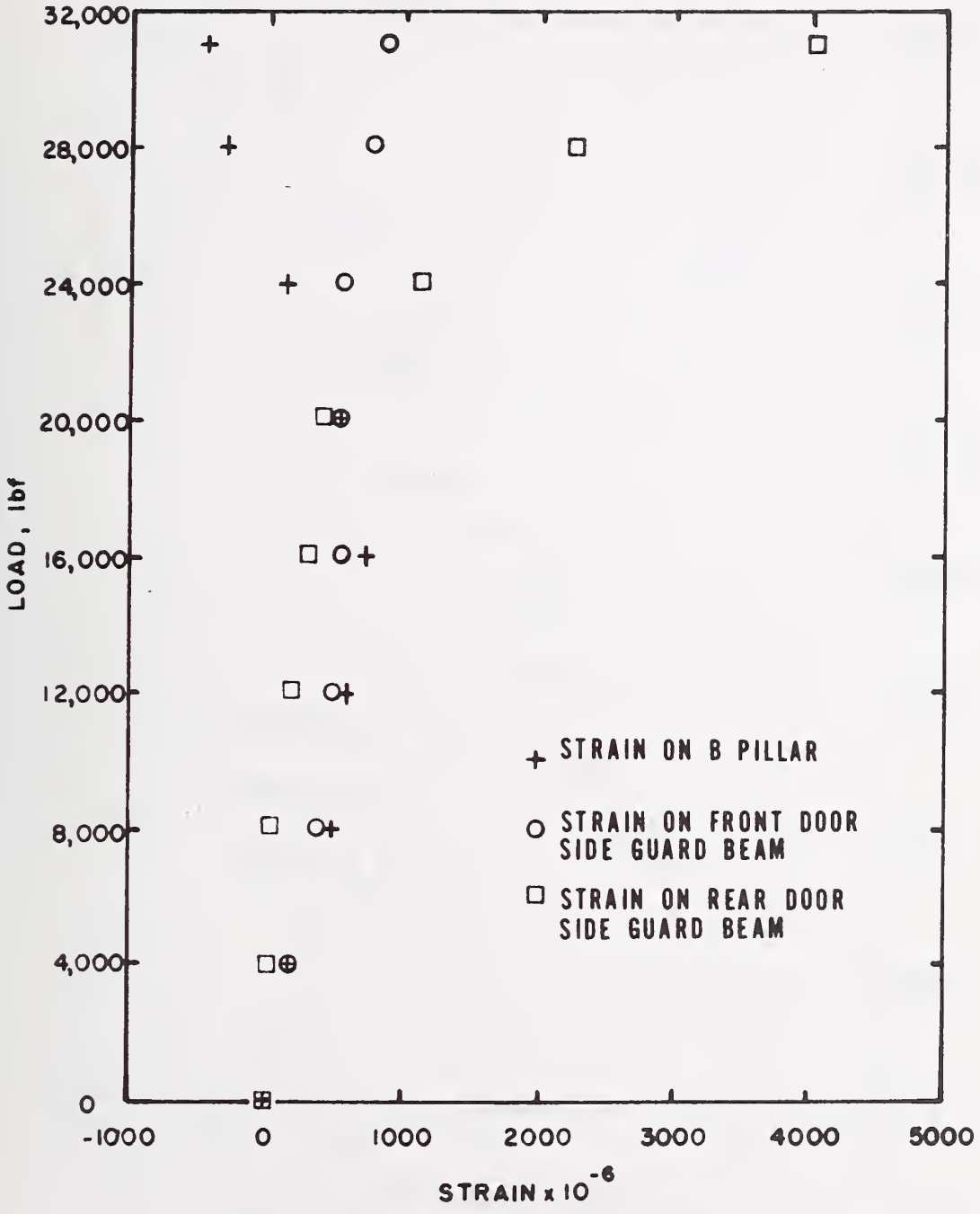

Figure 11 – LOAD VERSUS STRAIN AT SEVERAL LOCATIONS ON SIDE STRUCTURE DURING STATIC CRUSH TEST OF VEHICLE B1

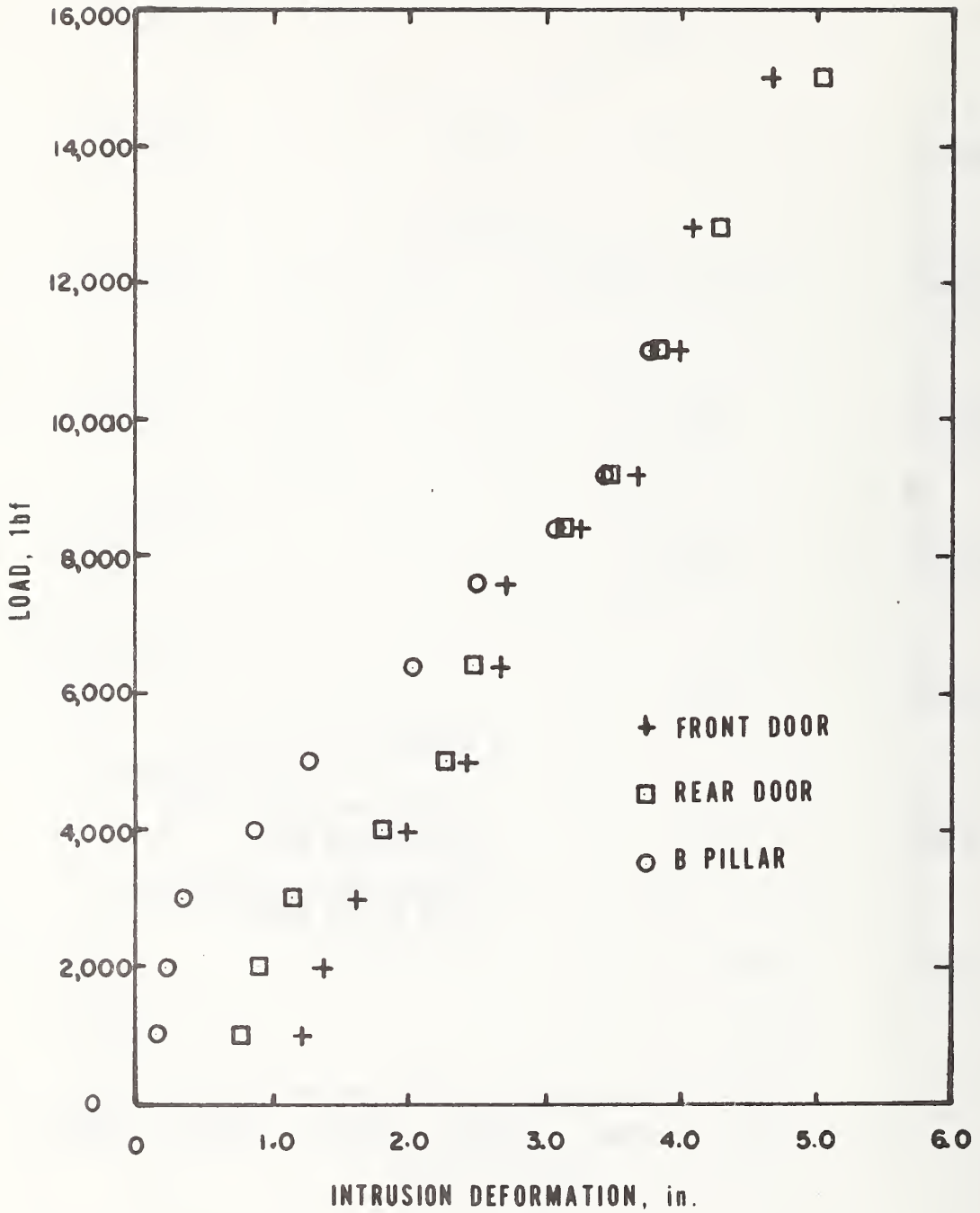

Figure 12 – LOAD VERSUS DEFORMATION AT THREE LOCATIONS ON THE LEFT SIDE OF VEHICLE A

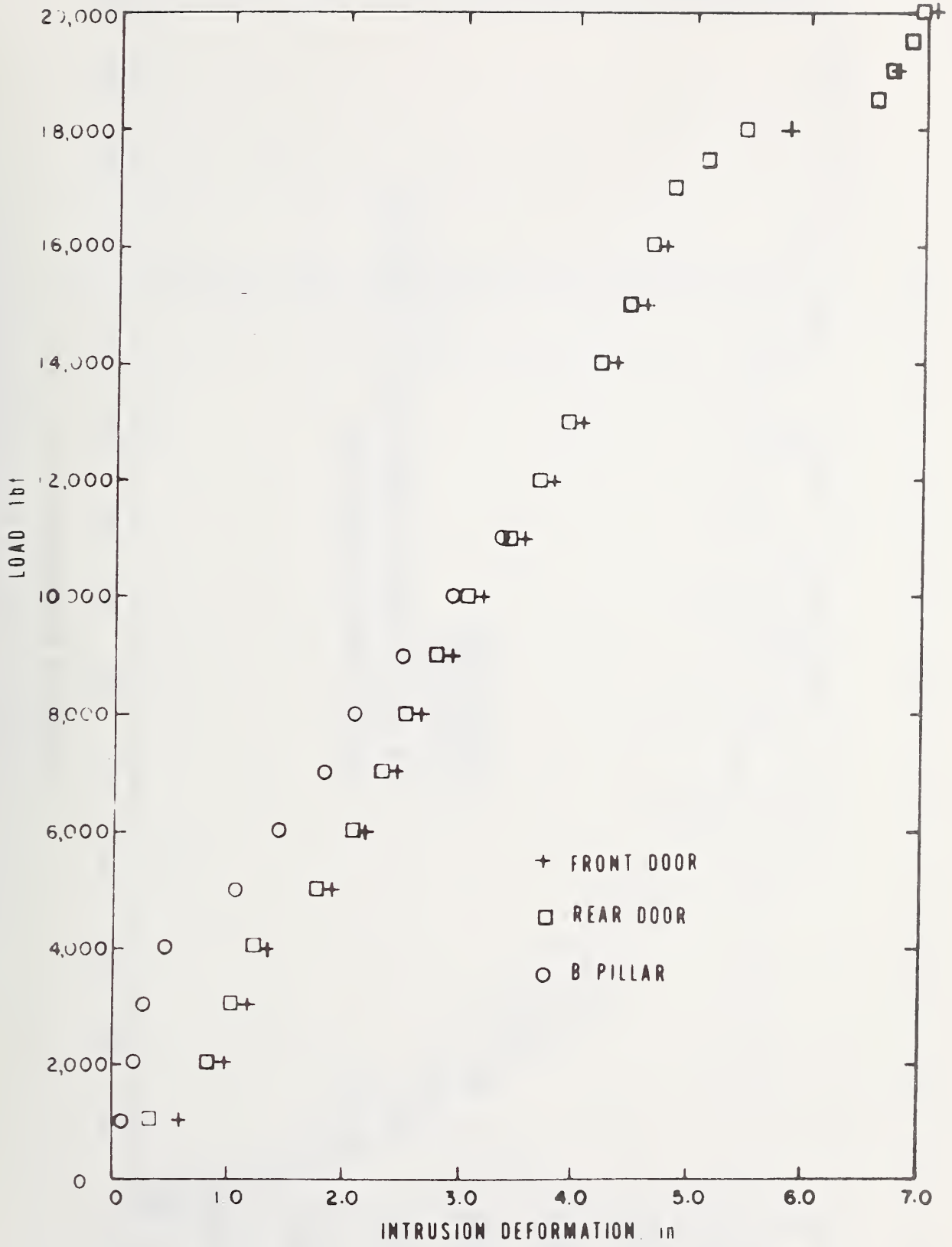

Figure 13 – LOAD VERSUS INTRUSION DEFORMATION AT THREE LOCATIONS ON THE RIGHT SIDE OF VEHICLE A

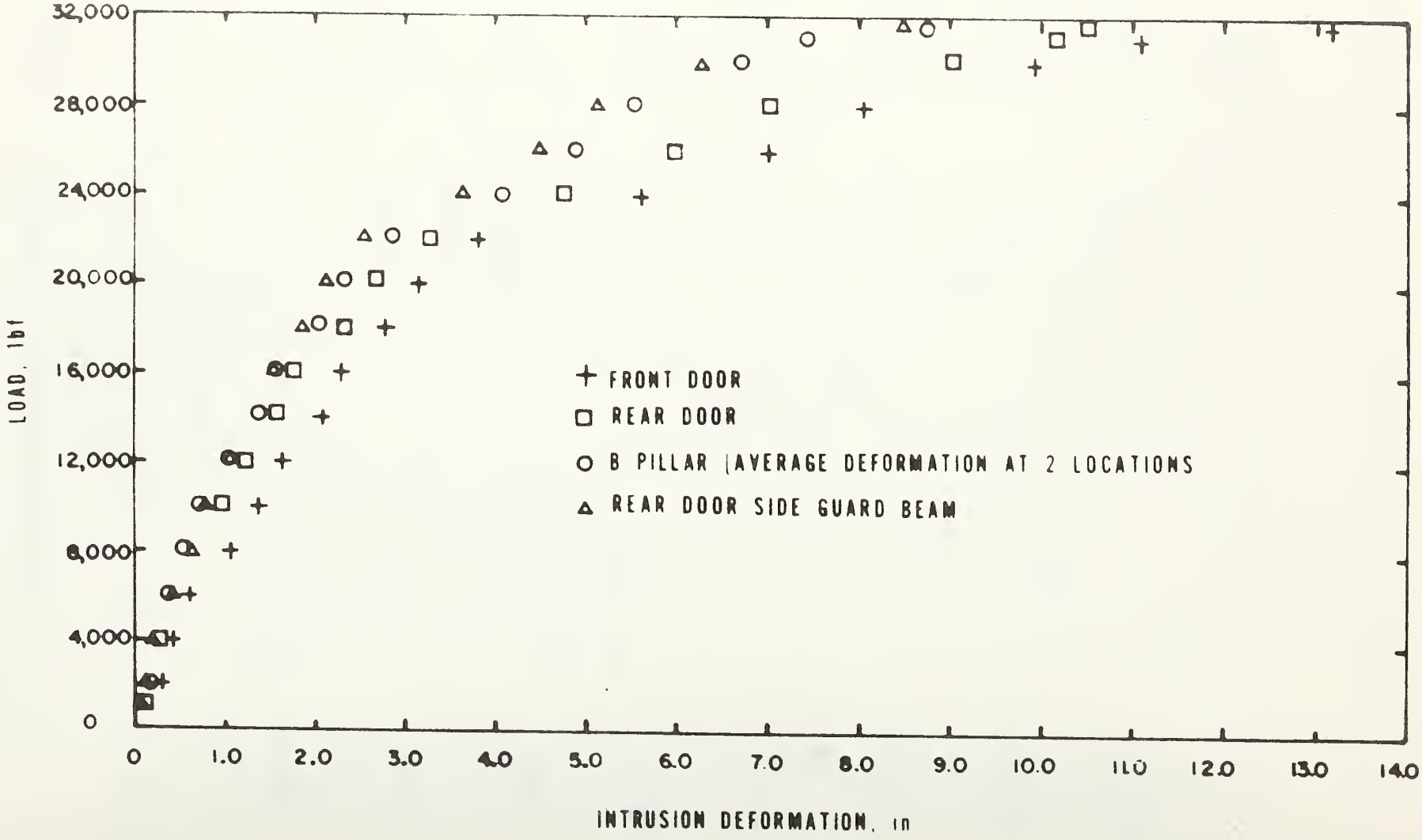

Figure 14— LOAD VERSUS DEFORMATION OF SIDE DOOR STRUCTURE FOR VEHICLE B1 LEFT SIDE

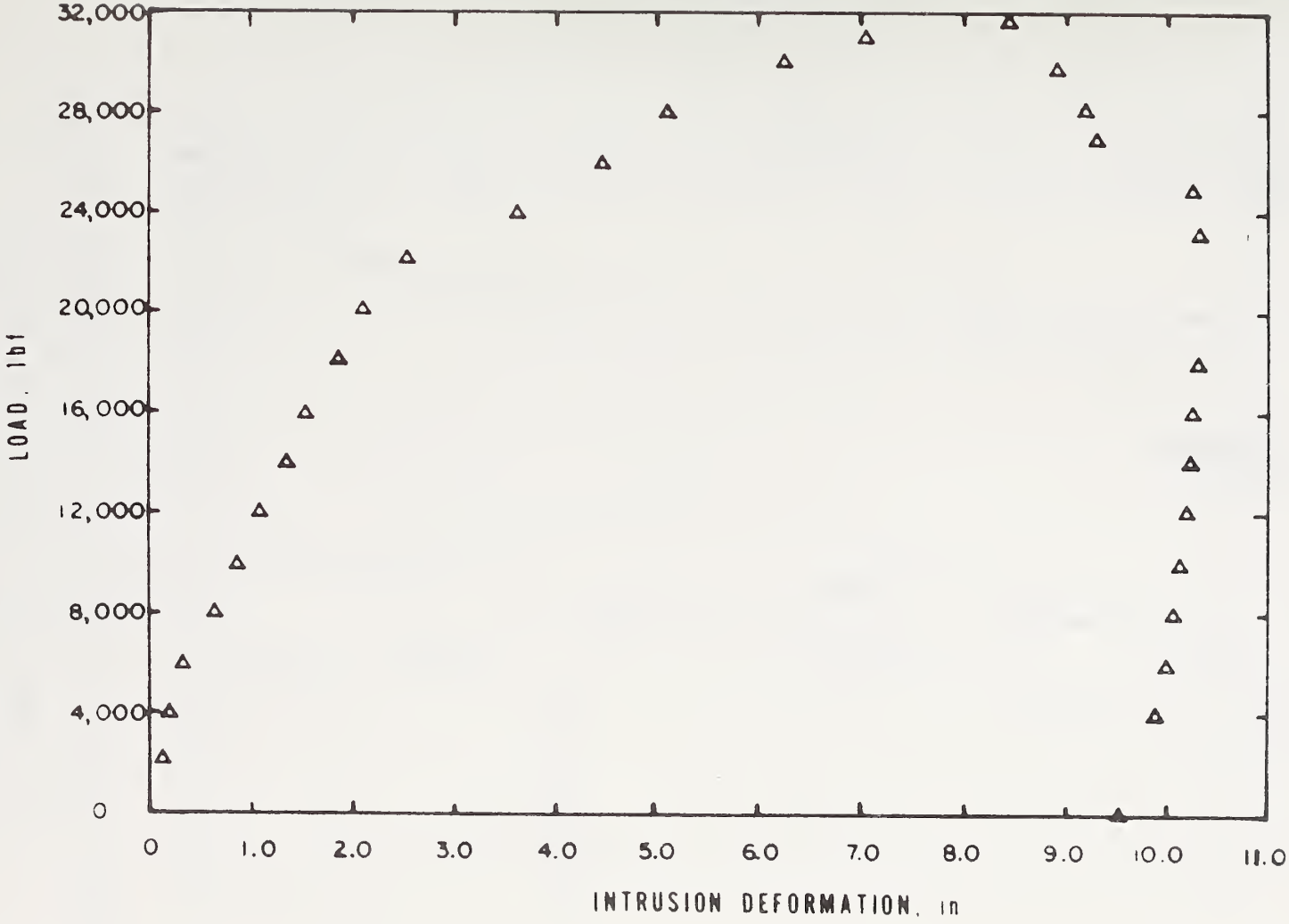

Figure 15 – LOAD VERSIS DEFORMATION OF DOOR SIDE GUARD BEAM FOR VEHICLE B1 LEFT SIDE

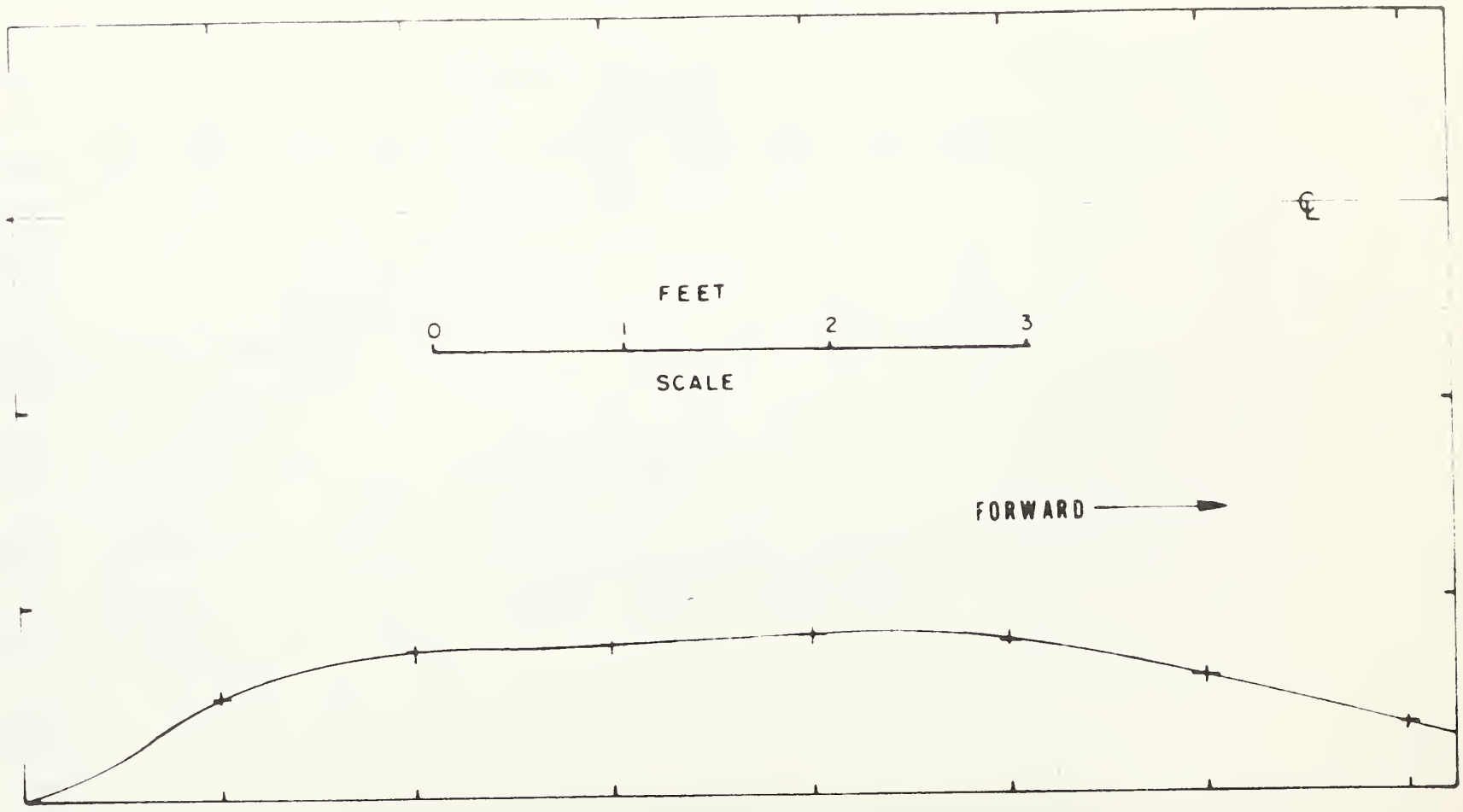

Figure 16 – EXTERNAL DEFORMATION OF VEHICLE A RIGHT SIDE IN LINE WITH SRP AFTER STATIC CRUSH TEST

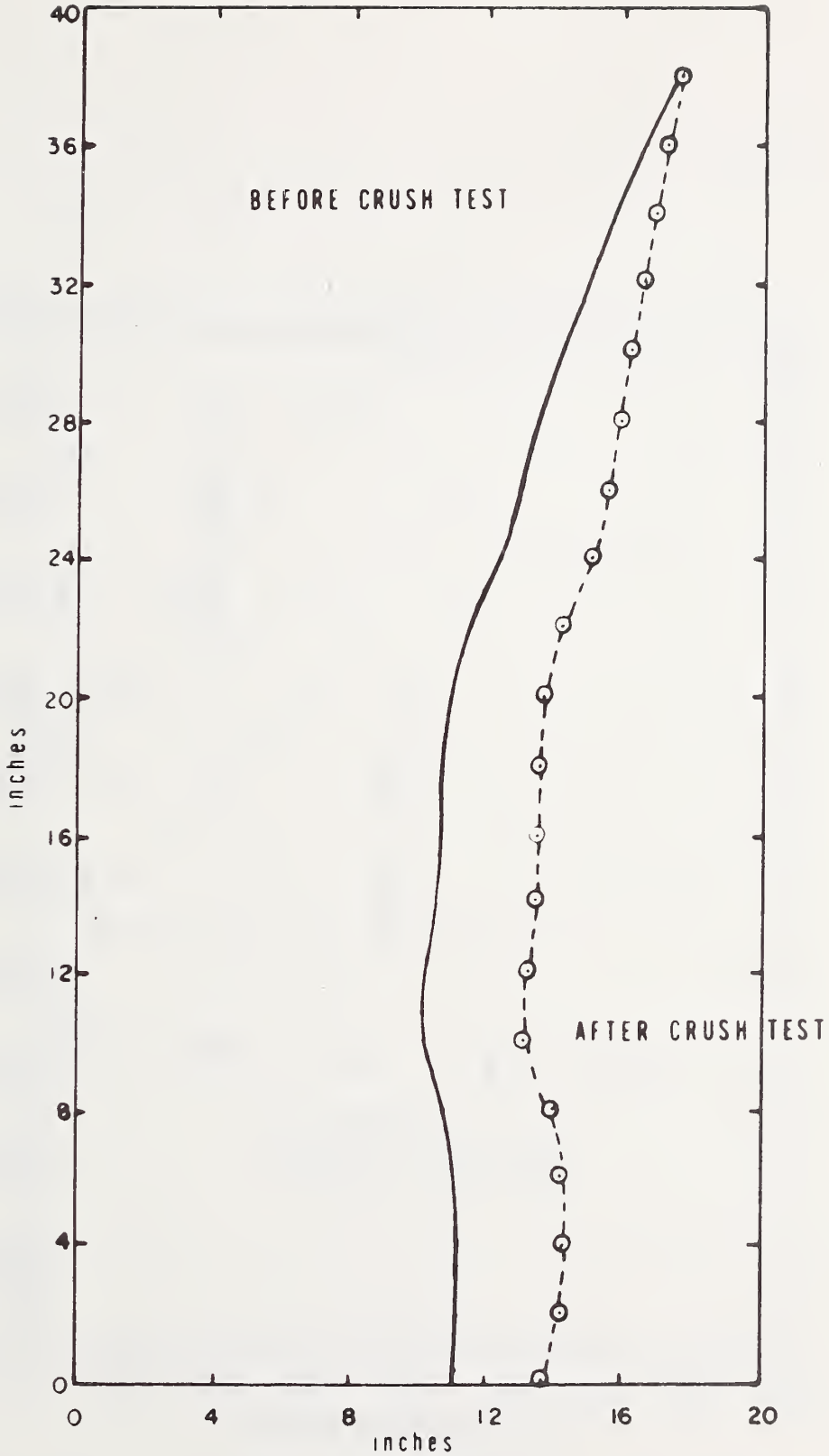

Figure 17 – VERTICAL PROFILE OF B PILLAR FOR VEHICLE A RIGHT SIDE BEFORE AND AFTER STATIC CRUSH TEST

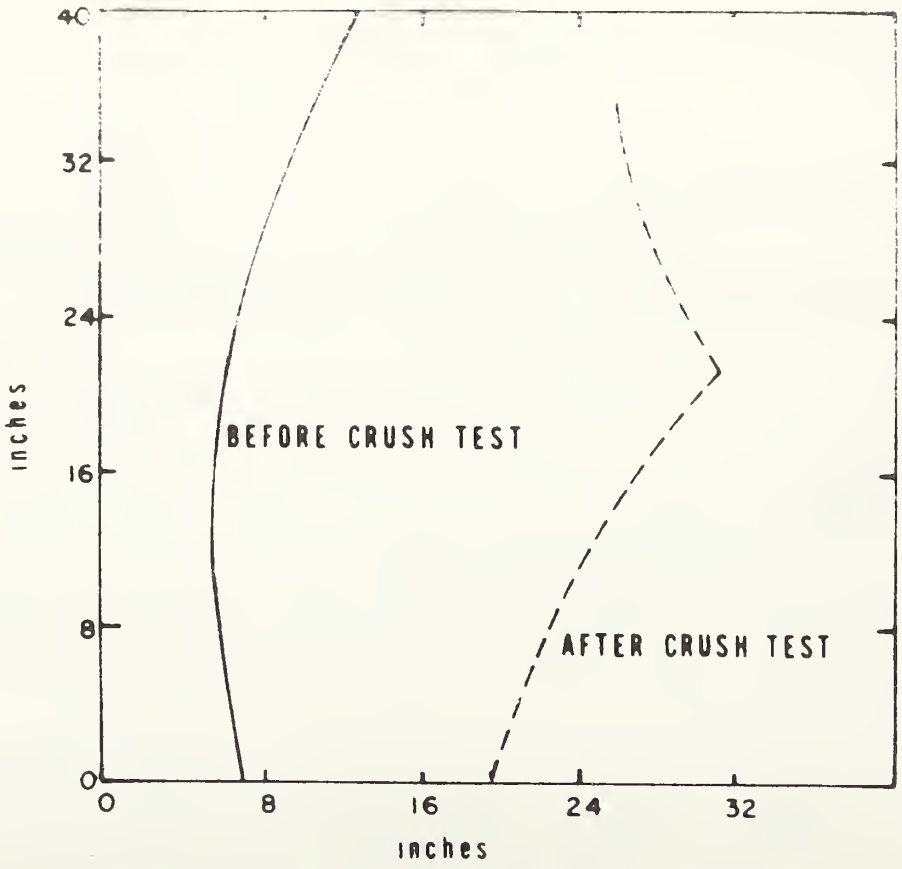

Figure 18 – VERTICAL PROFILE OF B PILLAR FOR VEHICLE B–1 LEFT SIDE BEFORE AND AFTER STATIC CRUSH TEST

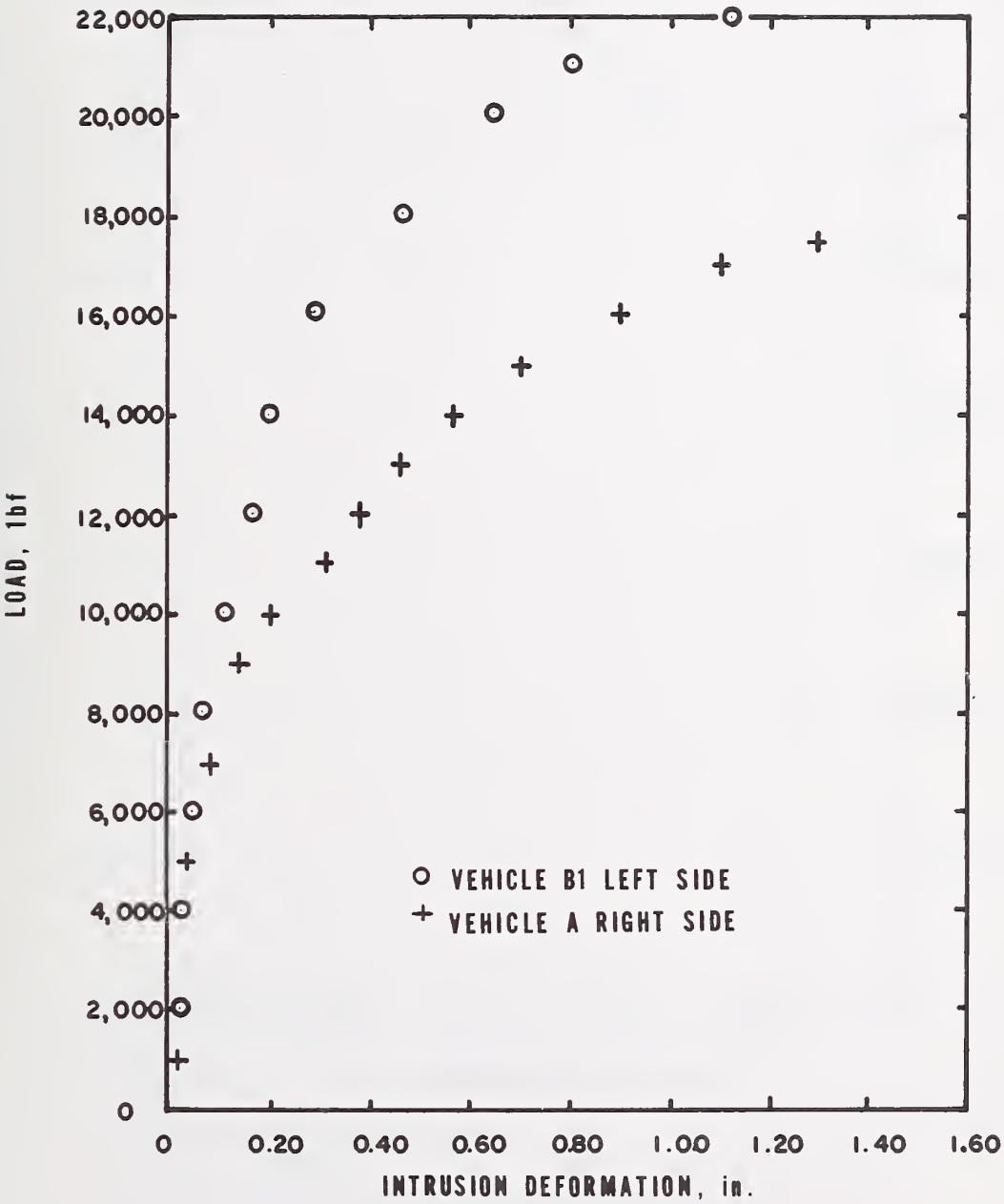

Figure 19 -LOAD VERSUS DEFORMATION OF A PILLAR DURING STATIC CRUSH TEST VEHICLES A & B1

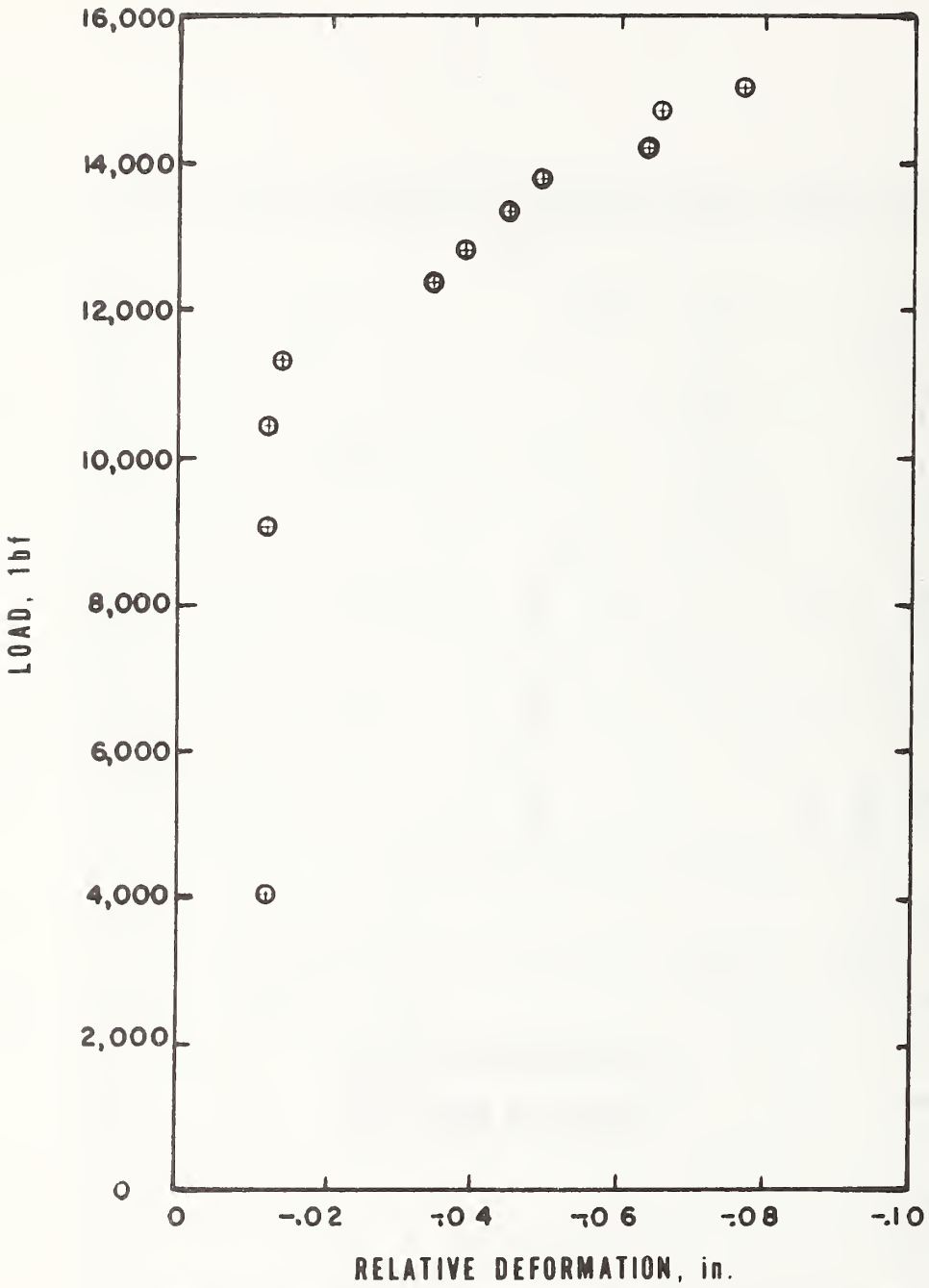

Figure 20 – RELATIVE DEFORMATION BETWEEN A AND B PILLARS VERSUS STATIC CRUSH LOAD ON VEHICLE A LEFT SIDE

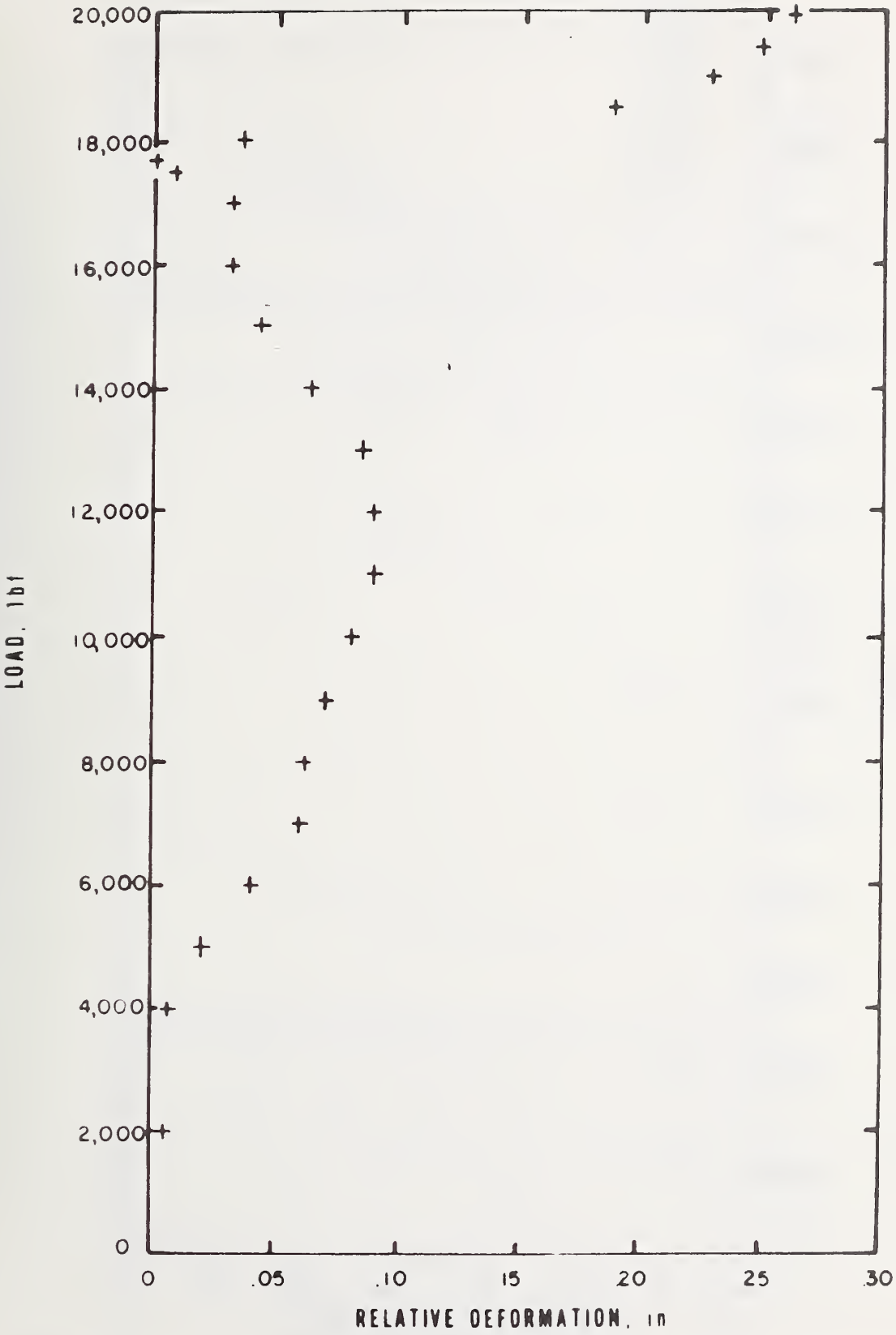

Figure 21 – RELATIVE DEFORMATION BETWEEN B AND C PILLARS VERSUS STATIC CRUSH LOAD ON VEHICLE A RIGHT SIDE

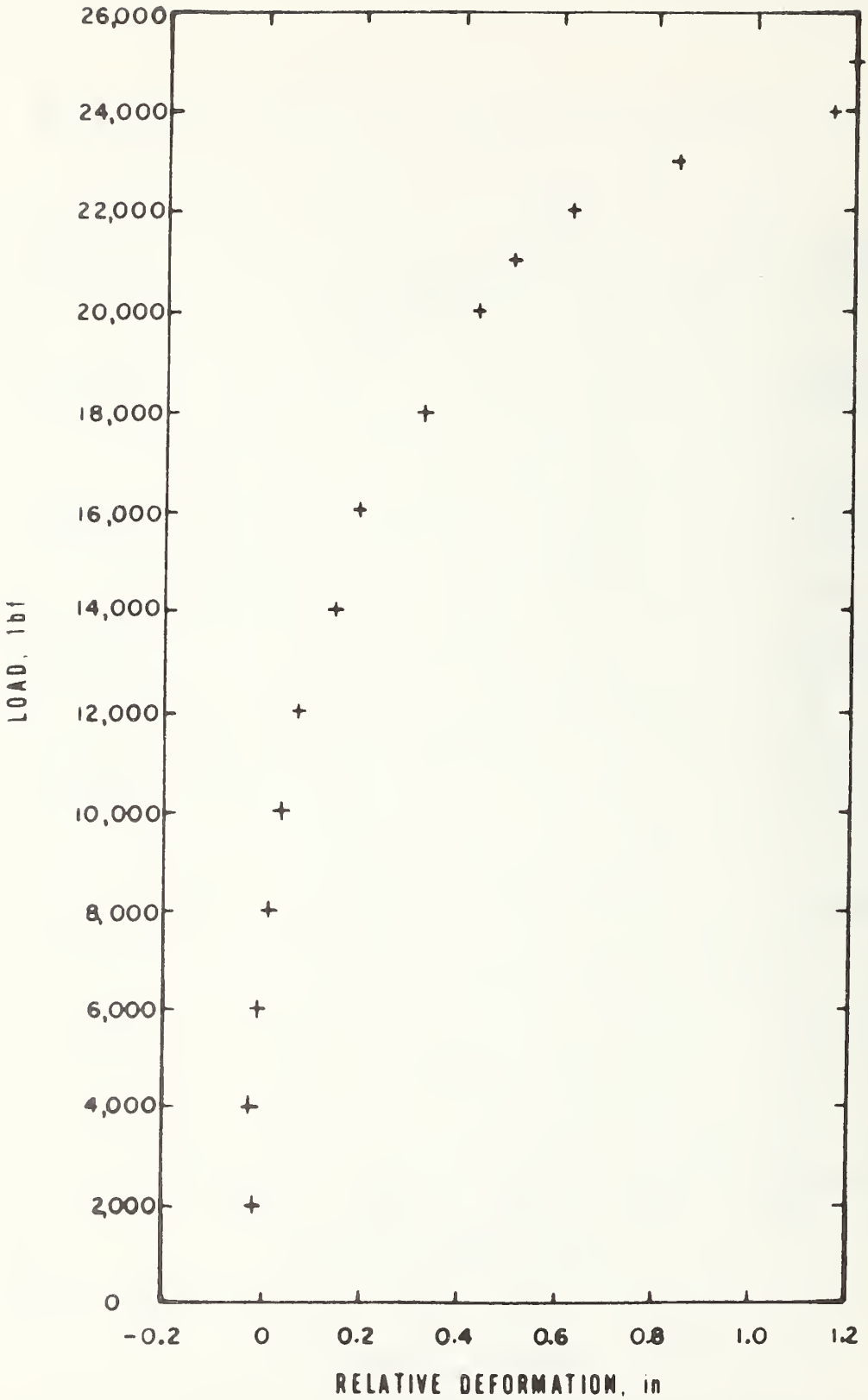

Figure 22 – RELATIVE DEFORMATION BETWEEN B AND C PILLARS VERSUS STATIC CRUSH LOAD FOR VEHICLE B1 LEFT SIDE

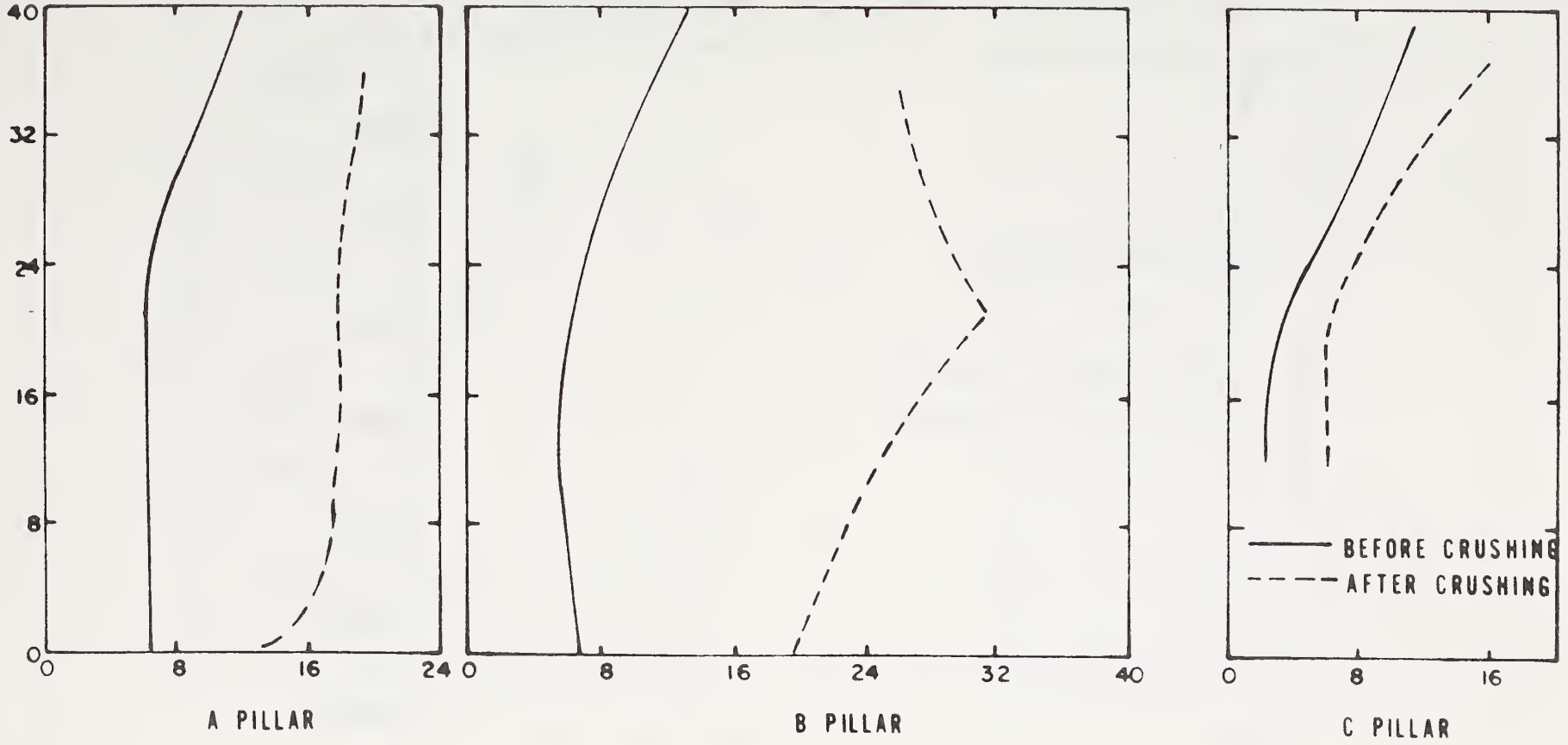

Figure 23 – VERTICAL PROFILE OF PILLARS FOR VEHICLE B1 LEFT SIDE BEFORE AND AFTER STATIC CRUSH TEST

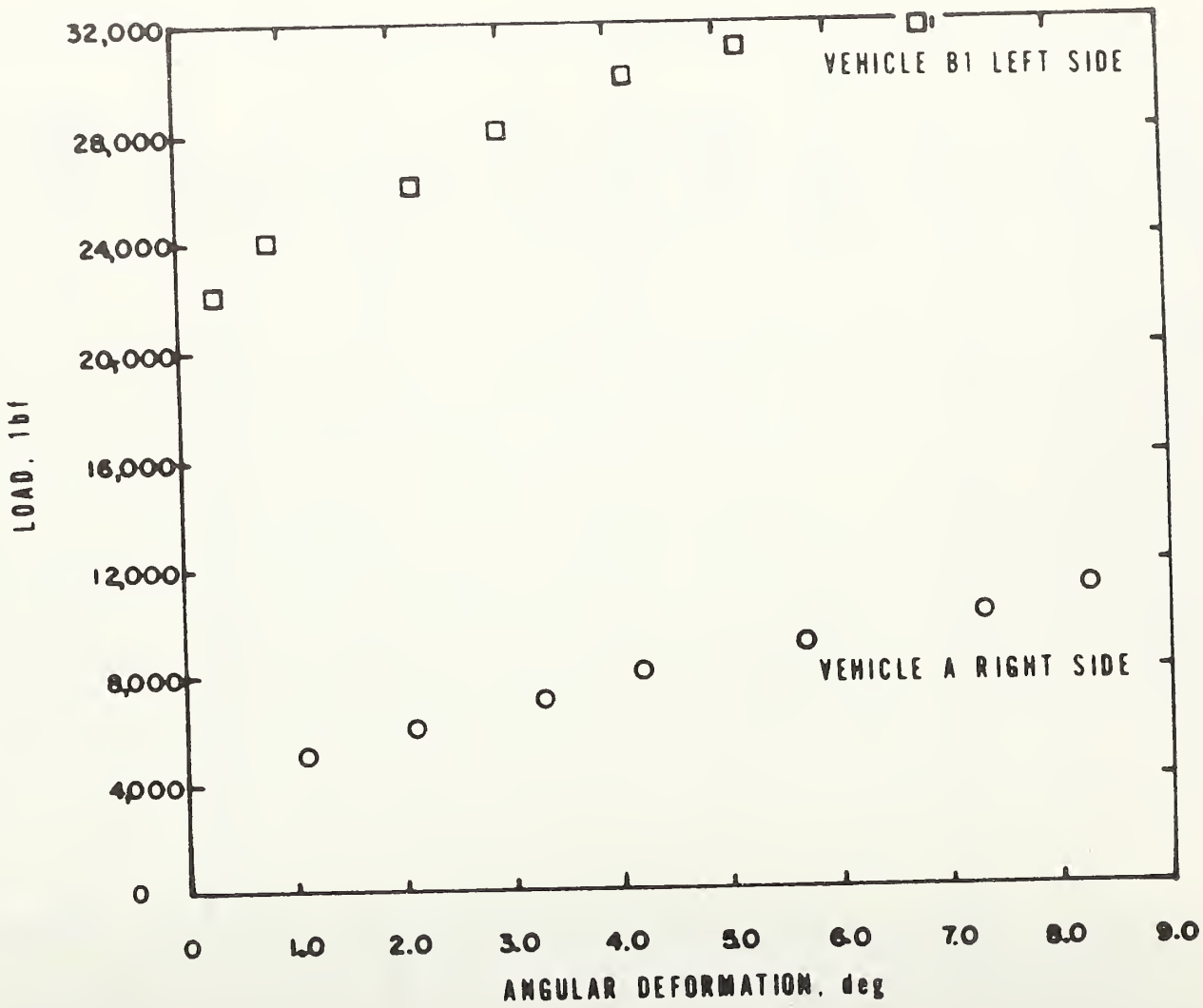

Figure 24 – ANGULAR DEFORMATION OF B PILLAR FOR VEHICLES A AND B1

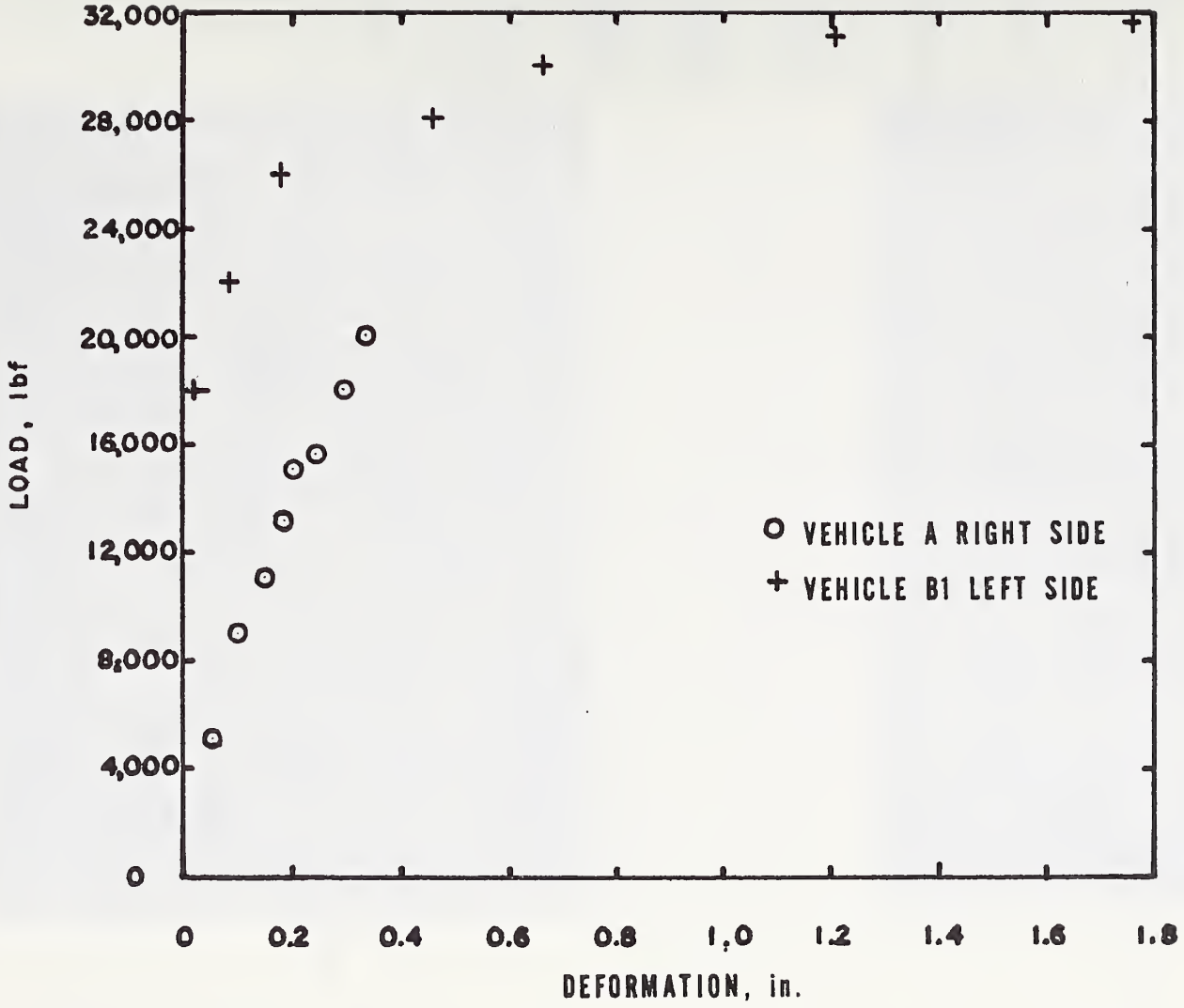

Figure 25 – LOAD VERSUS DEFORMATION AT FIREWALL FOR VEHICLES A AND B1

Figure 26 – FIREWALL FOR VEHICLE "B-1" BEFORE (UPPER) AND AFTER (LOWER) STATIC CRUSH TEST

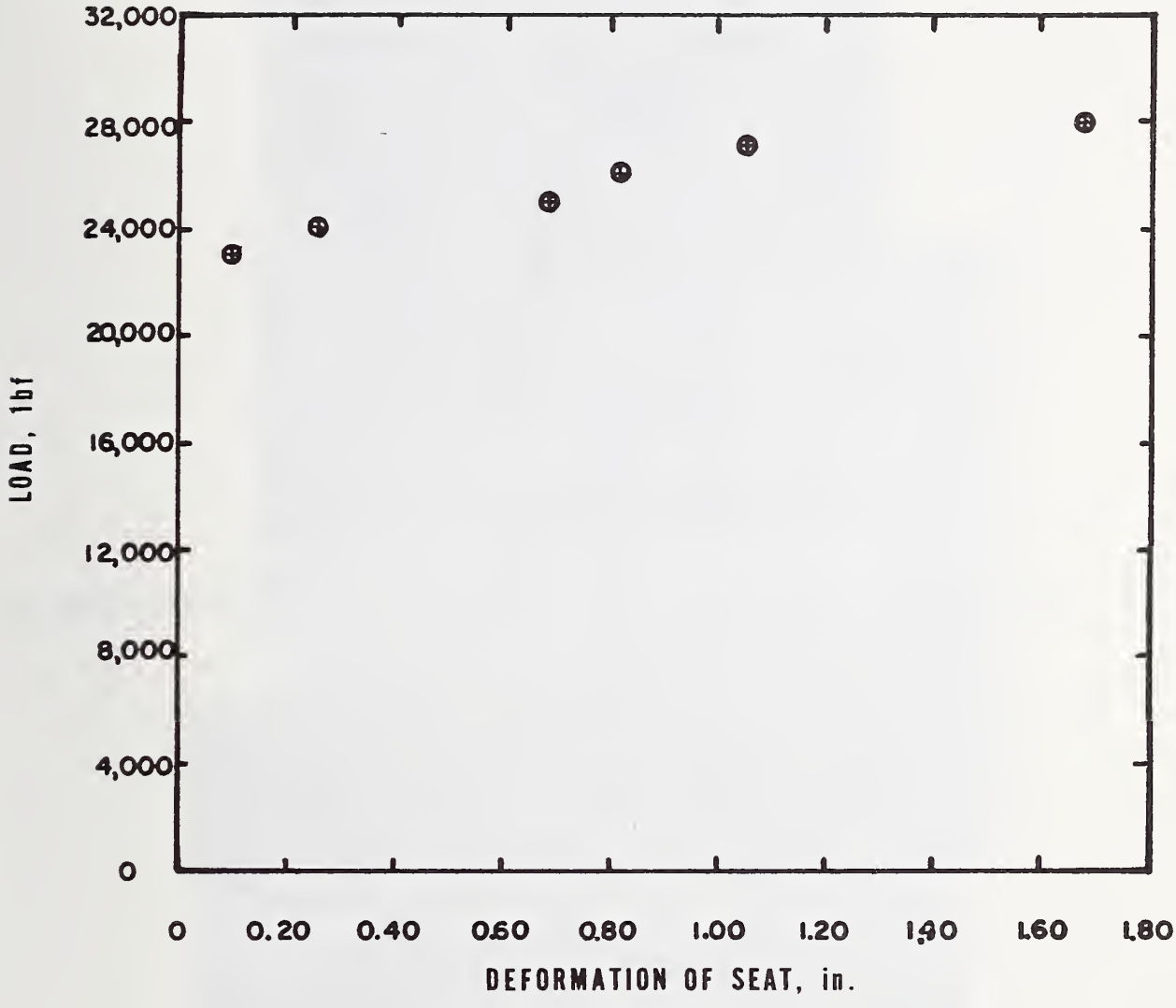

Figure 27 – DEFORMATION OF FRONT SEAT DURING CRUSH TEST OF VEHICLE B1 LEFT SIDE

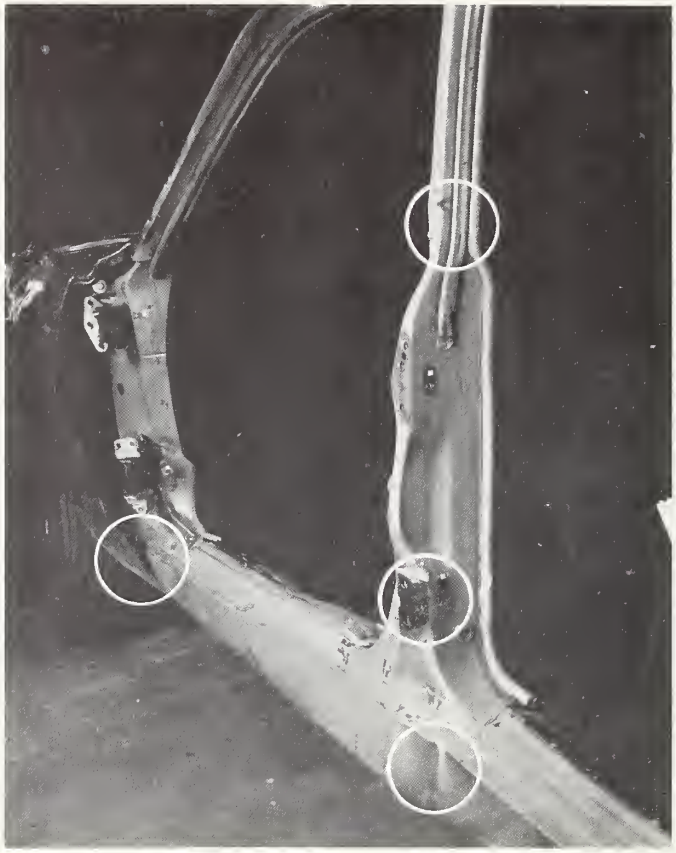

Figure 28 - REGIONS OF LOCAL DEFORMATION FOR VEHICLE "A" AFTER STATIC CRUSH TEST

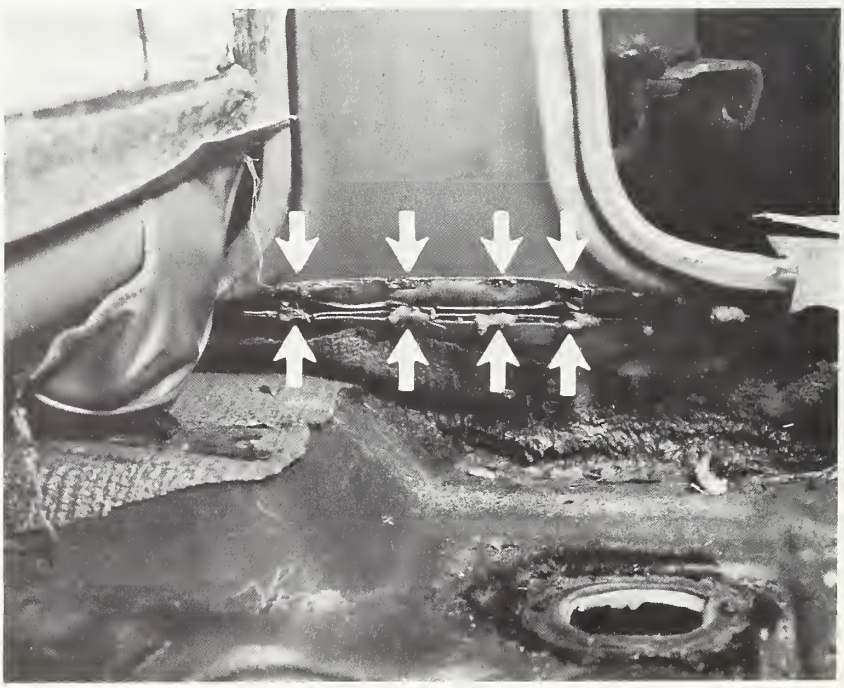

Figure 29 - FRACTURE OF WELDED JOINTS AT BASE OF B PILLAR AFTER STATIC CRUSH TEST OF VEHICLE "A- RIGHT SIDE

Figure 30 – BUCKLING DEVELOPED IN DASH DURING STATIC CRUSH TEST OF VEHICLE ''A''

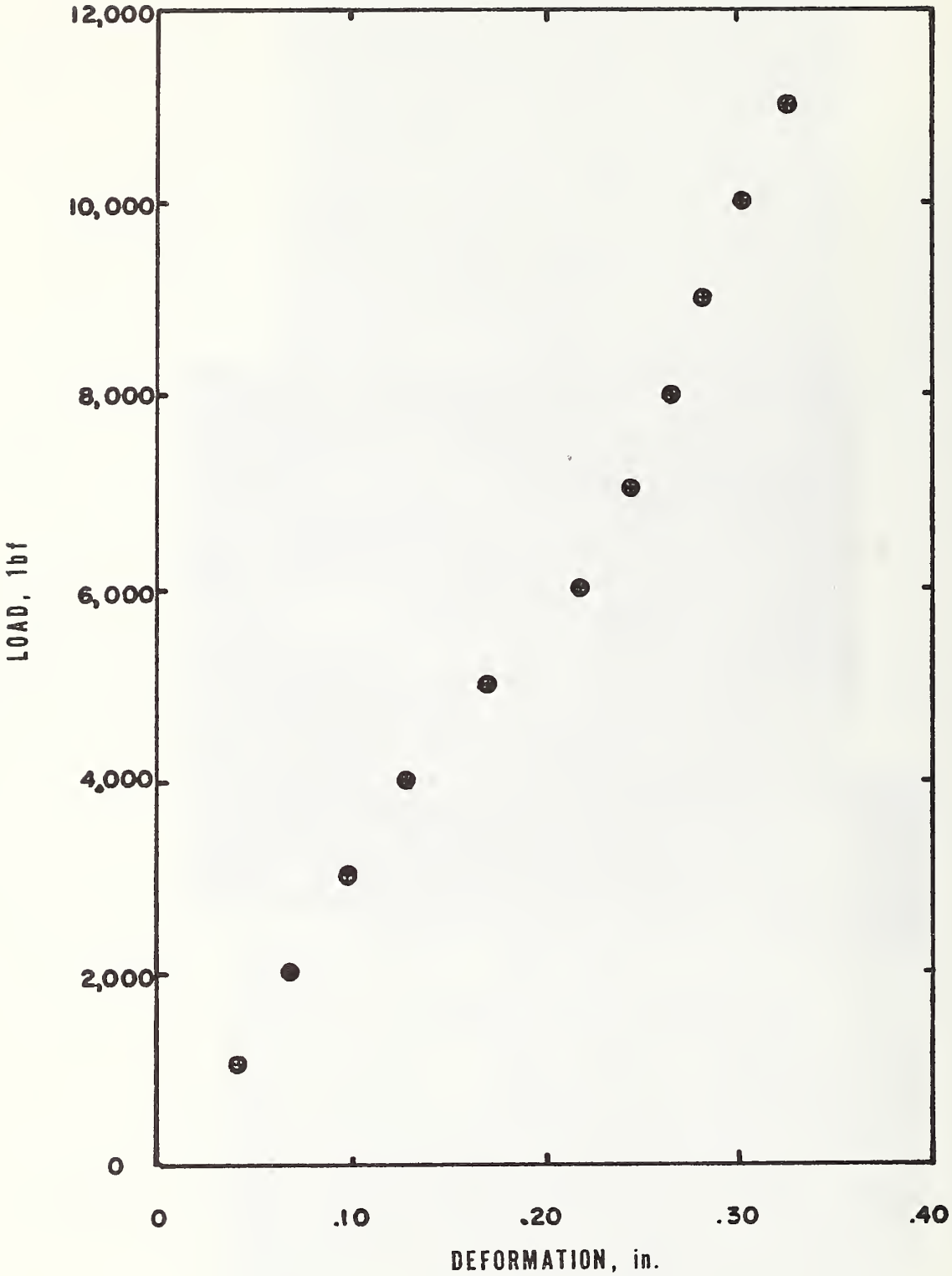

Figure 31 — DEFORMATION BETWEEN B PILLARS VERSUS LOAD FOR CRUSH TEST OF VEHICLE A RIGHT SIDE

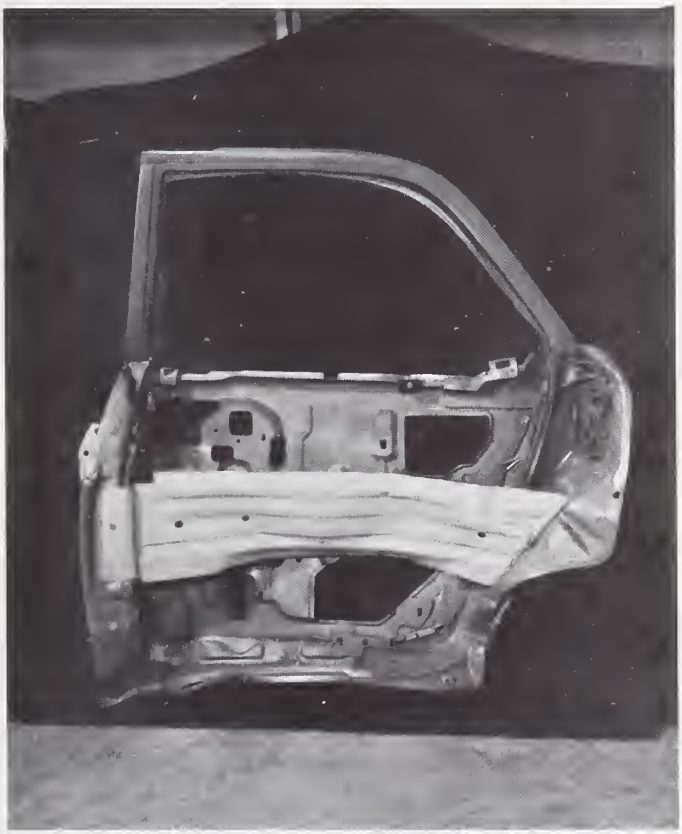

Figure 32 – DEFORMATION OF REAR DOOR SIDE GUARD BEAM AFTER STATIC CRUSH TEST OF VEHICLE "B-1"

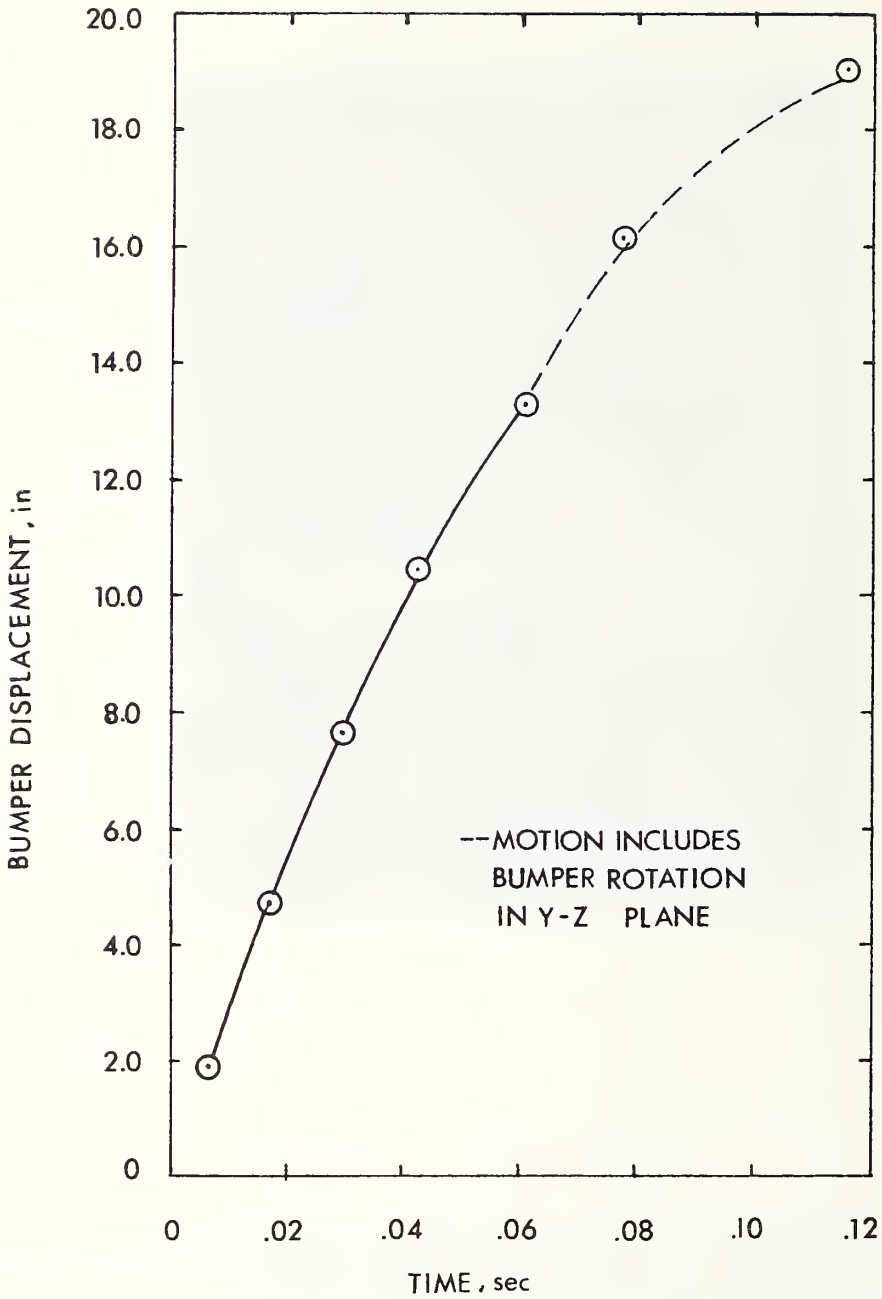

Figure 33 BUMPER DISPLACEMENT VERSUS DURATION OF IMPACT FOR DYNAMIC CRUSH TEST OF VEHICLE C-1

Figure 34 - EXTERNAL SIDE DEFORMATION AFTER STATIC TEST OF VEHICLE "B-1" (UPPER) AND DYNAMIC TEST OF VEHICLE "B-2" (LOWER)

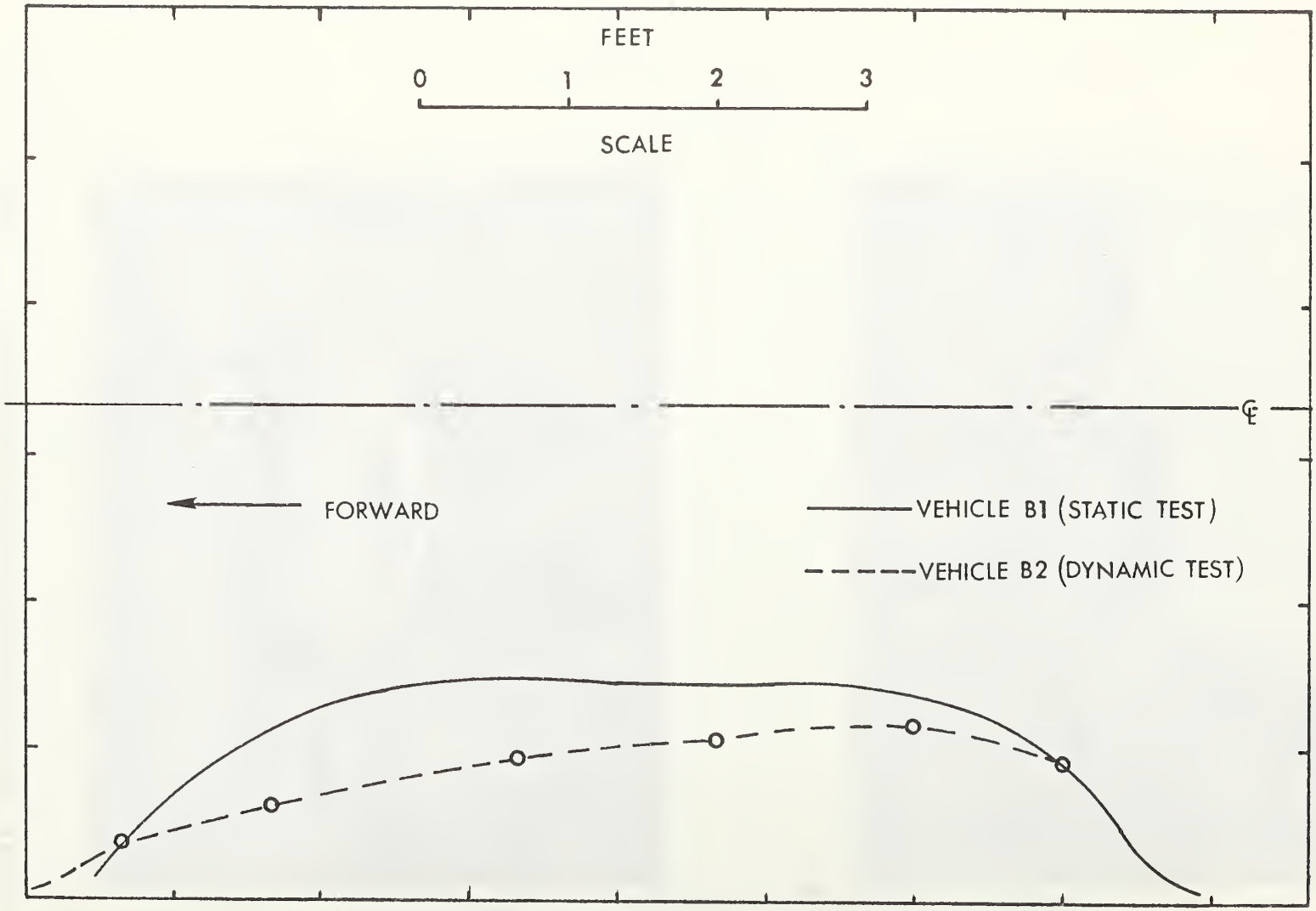

Figure 35 VEHICLE EXTERNAL SIDE DEFORMATION IN LINE WITH SRP AFTER STATIC AND DYNAMIC CRUSH TESTS

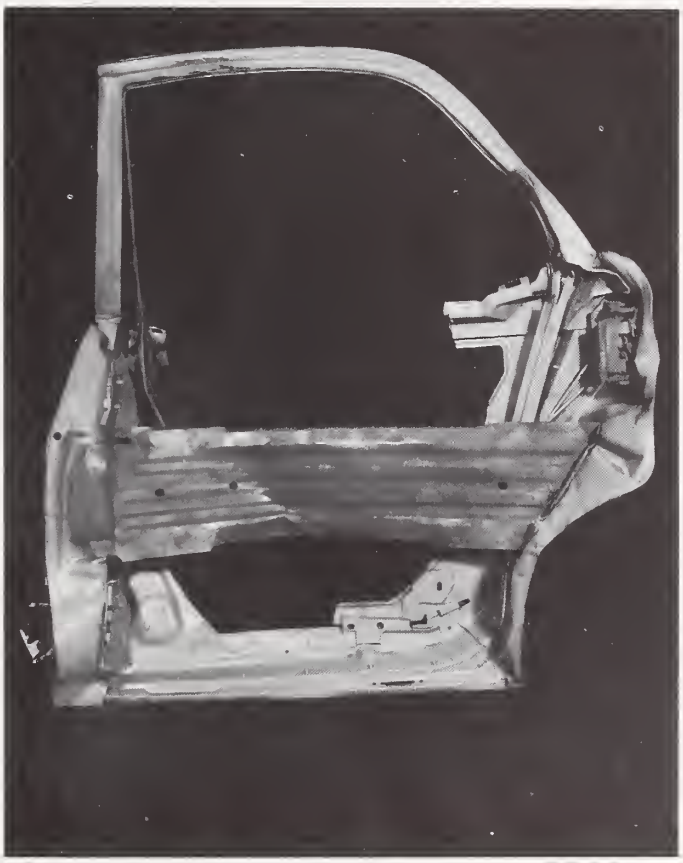

Figure 36 – DEFORMATION OF REAR DOOR SIDE GUARD BEAM AFTER DYNAMIC CRUSH TEST OF VEHICLE "B-2"